Czech Technical University in Prague
Faculty of Electrical Engineering
Department of control engineering

The use of Radon transform in medicine and biology

Bachelor thesis

Marija Pajdaković

Field of study: Cybernetics and Robotics
Supervisor: doc. RNDr. Jiří Velebil, Ph.D.

Prague, 2022

BACHELOR'S THESIS ASSIGNMENT

I. Personal and study details

Student's name: **Pajdaković Marija** Personal ID number: **492351**

Faculty / Institute: **Faculty of Electrical Engineering**

Department / Institute: **Department of Control Engineering**

Study program: **Cybernetics and Robotics**

II. Bachelor's thesis details

Bachelor's thesis title in English:

The use of Radon transform in medicine and biology

Bachelor's thesis title in Czech:

Použití Radonovy transformace v medicíně a biologii

Guidelines:

Radon transform (invented in 1917) allows one to recover a function on a region of plane, knowing integrals of its values along the lines. This property is a mathematical foundation of modern imaging methods in medicine and elsewhere, known as Computer Tomography (CT). The thesis will give a slight overview of CT and it will focus on the reconstruction problem of Radon transform, aka the inverse Radon transform. The core of the thesis will thus consist of the proof of The Central Slice Theorem. The theory will be explained on simple examples.
The style and presentation of the thesis will be theoretical, maintaining mathematical standards.

Bibliography / sources:

[1] Charles L Epstein, Introduction to the mathematics of medical imaging, 2nd ed, SIAM, 2008.
[2] Timothy G Feeman, The mathematics of medical imaging, 2nd ed, Springer, 2015.
[3] Paul Suetens, Fundamentals of medical imaging, 2nd ed, Cambridge University Press, 2009.

Name and workplace of bachelor's thesis supervisor:

doc. RNDr. Jiří Velebil, Ph.D. Department of Mathematics FEE

Name and workplace of second bachelor's thesis supervisor or consultant:

Date of bachelor's thesis assignment: **21.01.2022** Deadline for bachelor thesis submission: **20.05.2022**

Assignment valid until:
by the end of summer semester 2022/2023

doc. RNDr. Jiří Velebil, Ph.D.	prof. Ing. Michael Šebek, DrSc.	prof. Mgr. Petr Páta, Ph.D.
Supervisor's signature	Head of department's signature	Dean's signature

III. Assignment receipt

The student acknowledges that the bachelor's thesis is an individual work. The student must produce her thesis without the assistance of others, with the exception of provided consultations. Within the bachelor's thesis, the author must state the names of consultants and include a list of references.

.	
Date of assignment receipt	Student's signature

Declaration

I hereby declare that I completed the presented thesis independently and that all used sources are quoted in accordance with the Methodological Instructions that cover the ethical principles for writing an academic thesis.

In Prague, 2022

.....
Marija Pajdaković

Acknowledgements

First and foremost, I would like to express my gratitude to the supervisor of the thesis, doc. RNDr. Jiří Velebil, Ph.D.. Thank You for all the knowledge, patience, and time shared selflessly with me. Most of all, thank You for a big motivation, which was one of the main factors for the successful completion of the thesis.
Special gratitude goes to my mother Mira, father Velibor, sister Marina, and all of my friends for being along my side throughout my studies and making me the person I am today.

Abstract

The thesis focuses on the use of Radon Transform in Computerized Tomography (CT). After a brief technical description of CT, we turn to the Radon transform as the primary mathematical tool of CT. We state and prove the main results of the direct one-dimensional Radon transform. Finally, we show how to reconstruct the original function (i.e, how to obtain the Radon transform by using the Central slice theorem.)

Keywords: Computerized tomography, Radon transform, Fourier transform, Central slice theorem.

Abstrakt

Práce se soustřeďuje na použití Radonovy transformace v počítačové tomografii (CT). Po krátkém technickém popisu CT je pozornost obrácena k Radonově transformaci, jakožto hlavního matematického nástroje CT. Dokazujeme hlavní výsledky teorie Radonovy transformace v dimensi 1. Poté ukazujeme, jak rekonstruovat původní funkci pomocí Central slice theorem.

Klíčová slova:počítačová tomografie, Radonova transformace, Fourierova transformace, Central slice theorem.

Contents

List of Figures

List of Tables

Chapter 1

Introduction

Mathematics has many applications in our daily lives that we often are not even aware of. It has been used in technologies such as cellular telephones, satellite positioning systems, online banking, metal detectors [9] etc. Out of all its applications, it is certain that the most beautiful and profound one is its ability to save our lives. The application of mathematics in medicine is a really powerful tool not only in disease diagnosis but also in their treatment. One of these tools, necessary for modern medicine as we know it today, is medical imaging. Back in times when we did not know much about medical imaging and X-rays, every change/disease of our internal organs demanded invasive methods such as operations, often leading to unwanted complications and difficulties. The problems with such methods mainly occur in any brain examination because they are highly unsafe and can cause permanent brain damage. Techniques used in medical imaging are not invasive and can help us analyze our internal body and discover changes such as tumours, bone or teeth fractures, etc [22]. Today, a variety of medical imaging techniques are being used. Some of them use a source of radiation inside a body such as *magnetic resonance imaging* (MRI), *positron emission tomography* (PET) and *single photon emission computed tomography* (SPECT). The others use the source of radiation that is outside of a body, such as *X-rays* and *ultrasounds* [20]. The technique that uses X-rays is called *computerized axial tomography* (CAT or CT), whose main principles and ideas are going to be discussed in this thesis. The basic idea behind a CT scanner is to collect a lot of two-dimensional slices of a particular medium, and then use them to reconstruct a three-dimensional body. This problem is known today as an inverse problem and was studied by an Austrian mathematician Johann Radon back in 1917 [18]. After obtaining a body reconstruction, we can readily determine whether there are any changes and, if so, where they are located inside the body.

This thesis will discuss the main principles of tomography, the behavior of X-rays pass-

ing through the medium together with its mathematical model,the Radon transform, and finally, the inverse Radon transform. **Chapter 2** gives a sketchy overview how CT works. We discuss the behaviour of human tissue when exposed to X-rays. The mathematical description of this behaviour can be summarised in a differential equation called *Beer's law*. Since X-rays scan the tissue along lines in CT, we give a mathematical model that will allow us to treat those lines correctly. This model, along with a recapitulation of *line integrals*, is presented in **Chapter 3**. The basic properties of the Radon transform, the main tool of CT, is given in **Chapter 4**. In **Chapter 6** we come to the statement and proof of The Central slice theorem, which says that the Radon transform is invertible. This is a crucial result: it enables us to reconstruct the tissue from the slices obtained along the lines. Since the proof lingers upon multidimensional Fourier transform, we give necessary results on it in **Chapter 5**. Finally, in **Chapter 7** we discuss an example of the Central slice theorem. We indicate that even a simple function may involve non-trivial functions (the so-called *Bessel functions*). Thus, in practice, the reconstruction is mostly done by approximative numerical analysis methods.

Chapter 2

X-rays behaviour and tomography

In this chapter, we will say something about the tomography and the nature of X-rays as they pass through a medium such as human tissue.
We know that light is a form of electromagnetic radiation with different wavelengths. Some of those wavelengths appear to us as visible light, while others appear as radiation that we cannot see. Examples of those radiations are ultra-violet and infra-red radiation or X-rays. X-ray is a type of electromagnetic radiation with extremely short wavelengths (10^{-8} to 10^{-12} m) and high frequency ($3 \cdot 10^{16}$ to $3 \cdot 10^{18}$ Hz [8]). Their shortwave lengths make them invisible to the human eye, whereas their high energy allows them to pass through different kinds of media such as muscle, bone, or brain tissue. Because of this property, they are used in CT scanners.

2.1 CT scanners

CT scanner is a standard device used in medicine—it has a source (the point from where the X-rays are emitted) and a detector, which is usually some sensitive material, like a piece of film or a digital sensor. We can see an example of a CT scanner principle in Figure 2.1. The main idea behind a CT is to measure energy at the source (initial energy) and one at the detector (final energy) and then compute the difference between these two energies. This process is done for thousands of X-ray beams at loads of different angles, which means that the source is being rotated around a full circle. Let us explain this with a simple example: if we place a hand in front of a flashlight, it will cast a shadow on the wall behind us. In the same manner, the X-ray beam will cast a shadow on the detector, giving us a picture from the shadow.
When a single beam passes through the medium, part of its energy is absorbed by the medium and the other part passes through it. Knowing the differences between initial and final energy gives us information about the medium. This information is an important

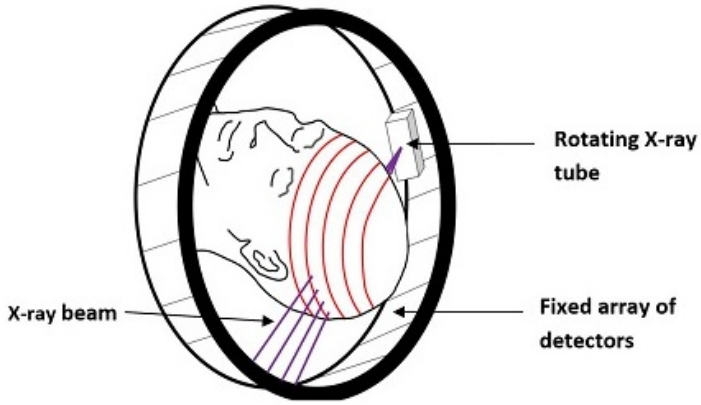

Figure 2.1: CT scanner principle [4]

property and we call it *attenuation coefficient*—it can be observed as a density of an object. Let us take an example of a bone fracture. Suppose that a CT scanner emits X-ray beams to the broken bone. The beam that passes through the part that is broken will be exposed by the digital sensor (detector), creating the picture of the medium, whereas the bone itself will absorb all others.

For a better understanding of this principle, let us represent a CT scanner as a simple grid model of black and white squares.

Example 2.1.1 (*Simple model of a CT principle* [10])**.** Suppose we have a medium represented as a 3-by-3 grid of black and white squares (see Figure 2.2), such that each white square absorbs one unit of energy, and the black square absorbs none. Hence, the black and white squares have different attenuation coefficients.

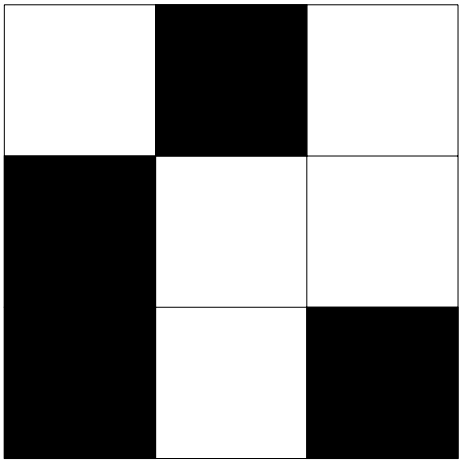

Figure 2.2: Medium represented as a grid of black and white squares

Our ultimate goal is to figure out the configuration of the grid by measuring the level of energy absorption by an X-ray passing through it. Let us assume that in the first measurement the family of parallel beams is perpendicular to the columns of the grid. One beam will lose two units of energy when passing through the first row, two units when passing through the second and one unit when passing through the third row. If we consider only the first row where X-ray loses two units of energy, we get three possible configurations, as shown in Figure 2.3

Figure 2.3: Possible configurations of the first row

In our second measurement, we will change the angle of the source to get some additional information about the medium. Let us choose an angle such that the beams are perpendicular to the rows of the grid. The X-ray will lose one unit of energy as it passes through the first column and two units through the second and the third column. We will use all of the information we gained to find all possible configurations of the first row and first column together. Knowing that the first row absorbs two units and the first column absorbs only one unit, we get four different possible solutions, as shown in Figure 2.4.

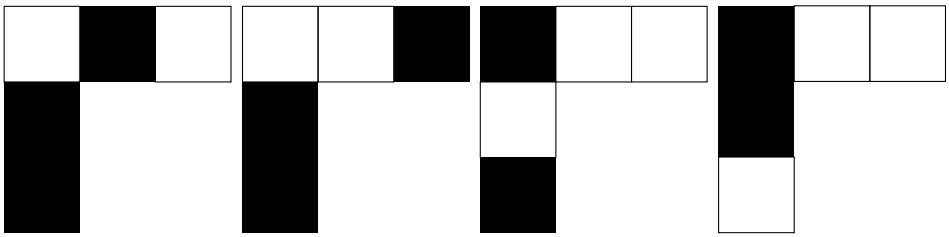

Figure 2.4: Possible configurations for first row and first column

Although we managed to reduce the initial 2^9 possible solutions to only 4, we still do not have all the information we require. Let us look at this from a slightly different point of view. Suppose we index the grid from x_1 to x_9. As pointed out above, the measurements of the loss in the intensity do not tell us the exact configuration of any row/column; it only tells us the overall loss of energy along them. We can represent this as a system with the matrix M such that it describes the loss of energy over every row

and every column. We can write it as follows:

$$\begin{pmatrix} 1&1&1&0&0&0&0&0&0 \\ 0&0&0&1&1&1&0&0&0 \\ 0&0&0&0&0&0&1&1&1 \\ 1&0&0&1&0&1&0&0&0 \\ 0&1&0&0&1&0&1&0&0 \\ 0&0&1&0&0&1&0&1&0 \end{pmatrix} \begin{pmatrix} x_1 \\ x_2 \\ x_3 \\ x_4 \\ x_5 \\ x_6 \\ x_7 \\ x_8 \\ x_9 \end{pmatrix} = \begin{pmatrix} 2 \\ 2 \\ 1 \\ 1 \\ 2 \\ 2 \end{pmatrix} \tag{2.1}$$

where the matrix above is our six by nine real matrix of the system, vector $\mathbf{x} \in \mathbb{R}^9$ is the unknown vector, and the vector on the right side tells us how the energies add up (it is, therefore, the information that we obtain by measuring). We see that the matrix M is not invertible, thus the system can not have a unique solution. We need three more beams at different angle, chosen as shown in Figure 2.5, where different colours represent different angles.

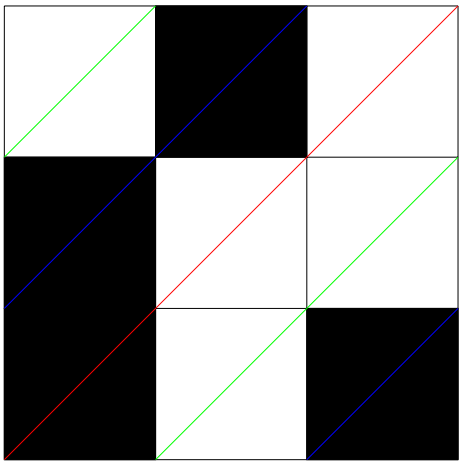

Figure 2.5: Three different beams represented as lines of three different colours

Writing these equations, we will have:

$$\begin{pmatrix} 1 & 0 & 0 & 0 & 0 & 1 & 0 & 1 & 0 \end{pmatrix} \begin{pmatrix} x_1 \\ x_2 \\ x_3 \\ x_4 \\ x_5 \\ x_6 \\ x_7 \\ x_8 \\ x_9 \end{pmatrix} = 3 \tag{2.2}$$

$$\begin{pmatrix} 0 & 1 & 0 & 1 & 0 & 0 & 0 & 0 & 1 \end{pmatrix} \begin{pmatrix} x_1 \\ x_2 \\ x_3 \\ x_4 \\ x_5 \\ x_6 \\ x_7 \\ x_8 \\ x_9 \end{pmatrix} = 1 \tag{2.3}$$

$$\begin{pmatrix} 0 & 1 & 0 & 0 & 1 & 0 & 1 & 0 & 0 \end{pmatrix} \begin{pmatrix} x_1 \\ x_2 \\ x_3 \\ x_4 \\ x_5 \\ x_6 \\ x_7 \\ x_8 \\ x_9 \end{pmatrix} = 0 \tag{2.4}$$

By adding these equations to the initial system (2.1), we get the real nine-by-nine matrix with the rank of 9, which has an inverse, and thus our solution for $\mathbf{x}$ is unique. This way we managed to find out the exact configuration of the grid by measuring the energy at several different angles.

The function in the example above was given as a discrete function. We had values $M(x_1)$, $M(x_2)$, ..., $M(x_9)$ from which we have found values of x_1, ..., x_9. In general, we want to solve this problem continuously, which is impossible since our number of given samples

will always be finite. That is why we need a wide range of samples at different angles, which will give us an accurate approximation.

2.2 Tomography

Tomography is a common technique used in medical imaging. The word comes from the Greek word *tomos* which means *cut* or *slice* [20]. The term *slice* describes the reconstruction of a three-dimensional object such as an organ, given its two-dimensional slices that we measure externally with our CT scanner. As we have already mentioned in Section 2.1, the attenuation coefficient is a characteristic of a medium describing its ability to absorb energy. It is rather apparent that if we observe it as a density function, a bone will have a much higher coefficient than a muscle. In general, the value of the mentioned coefficient is non-negative. However, in tomography it is often expressed in Hounsfield[1] units, which compares the attenuation coefficient of medium and water. It is expressed by the following formula [10]:

$$H_{medium} = \frac{A_{medium} - A_{water}}{A_{water}}$$

where A is the true attenuation coefficient. In the table below, we can observe the values of attenuation coefficients for different human organs, expressed in Hounsfield units [10].

substance	Hounsfield units
bone	1000
liver	40 to 60
white matter	20 to 30
grey matter	37 to 45
blood	40
muscle	10 to 40
kidney	30
celebrospinal fluid	15
water	0
fat	-100 to -50
air	-1000

Table 2.1: Hounsfield units for some materials

Not only do different kinds of tissues have different coefficients. The coefficient differs, for example, in healthy and cancerous tissues as well [9] which is why it is a highly relevant factor in medical diagnosis.

[1] Godfrey Newbold Hounsfield and Allan McLeod Cormack were the first two engineers who developed CT scans, back in the 1960s [10].

Therefore, our goal is to find the values of the attenuation coefficient along the line path of an X-ray beam. In the later section, we are going to explain this in detail.

2.3 Beer's law

All definitions in this section can be found, with slightly different notation, in the book [9], unless stated otherwise.
Before we start to make a mathematical model of X-rays passing through the medium, we need to make certain assumptions about the nature of an X-ray. We think of X-rays as composed of particles called photons, and we assume that:

1. All X-ray beams are monochromatic, meaning that each photon propagates at the same frequency and has the same energy.

2. The width of an X-ray beam is zero.

3. Diffraction and refraction are not present — X-rays do not bend nor scatter when they come into contact with the medium.

It is important to mention that the assumptions stated above do not entirely correspond to reality. Since we are making a linear model, assumption 1. is necessary, but the consequences of its imprecision can cause different errors that are not going to be discussed in this thesis. When it comes to assumption 2., CT scanners often have corrective algorithms that deal with diffraction/refraction. As we have already mentioned, a beam is composed of photons, each having the same level of energy. Let us denote the energy at a point $\mathbf{x}$ as $E(\mathbf{x})$ and the number of photons per time unit passing through $\mathbf{x}$ as $N(\mathbf{x})$. Then the intensity $I(\mathbf{x})$ is

$$I(\mathbf{x}) = N(\mathbf{x}) \cdot E(\mathbf{x})$$

Considering a one-dimensional world, the intensity of the beam at point x would be $I(x)$, and the intensity at a point $x+\Delta x$ will be $I(x+\Delta x)$. Our interest is to find out the overall loss in intensity between these two points, which corresponds to the following formula:

$$I(x + \Delta x) - I(x) \approx -A(x) \cdot I(x) \cdot \Delta x \tag{2.5}$$

Let us consider a two-dimensional or a three-dimensional world, where X-rays are travelling along one-dimensional straight lines. For simplicity, we will consider only one line denoted by ℓ, that is given parametrically.

$$\ell = \{\mathbf{x}_0 + s \cdot \mathbf{v} \mid s \in \mathbb{R}\} \tag{2.6}$$

Then the intensity and the attenuation coefficient along this line are given as

$$i(s) = I(\mathbf{x}_0 + s \cdot \mathbf{v}) \tag{2.7}$$

$$a(s) = A(\mathbf{x}_0 + s \cdot \mathbf{v}) \tag{2.8}$$

Analogously to the equation (2.5) we get

$$i(s + \Delta s) - i(s) \approx -a(s) \cdot i(s) \cdot \Delta s \tag{2.9}$$

$$\Delta i(s) \approx -a(s) \cdot i(s) \cdot \Delta s \tag{2.10}$$

$$\frac{\Delta i(s)}{\Delta s} \approx -a(s) \cdot i(s) \tag{2.11}$$

Let $\Delta s \to 0$ and we get a differential equation known as **Beer's law**:

$$\frac{\mathrm{d}\, i(s)}{\mathrm{d}s} = -a(s) \cdot i(s) \tag{2.12}$$

Since (2.12) is a separable differential equation, we can write it as:

$$\frac{\mathrm{d}\, i(s)}{i(s)} = -a(s) \cdot \mathrm{d}s \tag{2.13}$$

Assume we are measuring the intensity of an X-ray between the points $\mathbf{x}_0 + b \cdot \mathbf{v}$ and $\mathbf{x}_0 + c \cdot \mathbf{v}$ of the line ℓ where $b, c \in \mathbb{R}$. Integrating (2.13) from $s = b$ to $s = c$ we get:

$$\int_b^c \frac{\mathrm{d}\, i(s)}{i(s)} = -\int_b^c a(s)\, \mathrm{d}s \tag{2.14}$$

$$\ln(i(c)) - \ln(i(b)) = -\int_b^c a(s)\, \mathrm{d}s \tag{2.15}$$

which gives

$$i(c) = i(b) \cdot e^{-\int_a^b a(s)\, \mathrm{d}s}$$

We will denote $i_0 = i(b)$ as the initial energy of the beam and $i_f = i(c)$ as the final energy, where both of them are known. What is unknown is the $a(s)$ — the *attenuation coefficient*, therefore, as we have concluded in (2.15), we can find the integral of the attenuation coefficient, but not the coefficient itself. The question about our ability to reconstruct the function within some constrictions (for example, some body), knowing the

values of integral along every line that passes through that body was Radon's motivation for his work.

Example 2.3.1 (*Example of Beer's law*)**.** Suppose we have a body in the Cartesian coordinate system whose attenuation coefficient we want to find. Let us say that our detector is in such a position that it emits X-rays perpendicularly to the y-axis, i.e., an X-ray beam is traveling along the x-axis from point $(1, 2)$ to point $(6, 2)$. Our measured intensities of the beam are the following:

$$i_0 = i(1) = 1$$

$$i_f = i(6) = e^{-1}$$

From (2.15) we have:

$$1 = \int_1^6 a(x)\,\mathrm{d}x \tag{2.16}$$

If we suppose that $a(x)$ is a constant function, we can solve given integral and get the attenuation coefficient $a = \frac{1}{5}$. In reality, $a(x)$ is not a constant function, which makes it difficult for us to find out what shape $a(x)$ has.

Chapter 3

Geometry of medical imaging

Since our main focus of interest will be to "collect information" along straight lines, we need a good representation of lines in the plane. Therefore, in section 3.1 we introduce such representation. Since by "collecting information" we mean integration, in section 3.2 we recall how line integrals are computed in general.
The material presented here is fairly standard. Our treatment of the space of lines is inspired by the book [6], and for the line integral, we refer to [1].

3.1 The space of lines in plane

As we saw in Chapter 2, our mathematical model of CT will be represented by measuring along lines, which are the paths of X-rays. In this section, we, therefore, introduce a convenient representation of those lines.
Every line ℓ in $\mathbb{R}^2$ can be described using Cartesian coordinate system by the following equation :

$$ax + by = c \tag{3.1}$$

where $a, b, c \in \mathbb{R}$ and $a^2 + b^2 \neq 0$. Rewriting (3.1) we get:

$$\frac{a}{\sqrt{a^2+b^2}}x + \frac{b}{\sqrt{a^2+b^2}}y = \frac{c}{\sqrt{a^2+b^2}}. \tag{3.2}$$

We can write (3.2) as a dot product of vectors (a, b) and (x, y), which yields

$$\langle \frac{(a,b)}{\|(a,b)\|}, (x,y) \rangle = \frac{c}{\|(a,b)\|} \tag{3.3}$$

Firstly, let us define t as $\frac{c}{\|(a,b)\|} = t$.
The point $(\frac{a}{\|(a,b)\|}, \frac{b}{\|(a,b)\|})$ lies on the unit circle and can be represented as a unit vector $\boldsymbol{\omega} = (\omega_1, \omega_2)$, which implies that $\boldsymbol{\omega} = (\cos\theta, \sin\theta)$, for $\theta \in [0, 2\pi)$. We are now able to

describe a line in the plane parametrised by t and θ as follows:

$$\ell_{t,\theta} = \{(x, y) \in \mathbb{R}^2 : \langle (x, y), \boldsymbol{\omega} \rangle = t\} \tag{3.4}$$

For a better understanding, we are going show this graphically (see Figure 3.1). Our unit

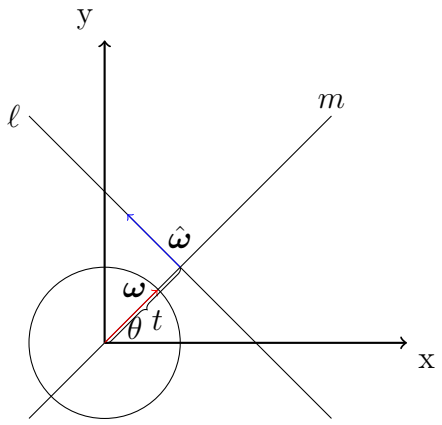

Figure 3.1: The parametrization of line $\ell_{t,\theta}$

vector $\boldsymbol{\omega} = (\cos\theta, \sin\theta)$ is perpendicular to the line $\ell_{t,\theta}$, as is the vector $t\boldsymbol{\omega}$. We notice that the point of intersection of the line $m = \{\boldsymbol{\omega}k : k \in \mathbb{R}\}$ and the line ℓ is a point $(t\cos\theta, t\sin\theta)$, where t is an affine parameter, i.e. it is a distance of the line ℓ from the origin. Let us define a unit vector $\hat{\boldsymbol{\omega}} = (-\sin\theta, \cos\theta)$ which is perpendicular to $\boldsymbol{\omega}$ and parallel to ℓ. Now we can describe our line only by t and θ as follows:

$$\ell_{t,\theta} = t\boldsymbol{\omega} + s\hat{\boldsymbol{\omega}} = (t\cos\theta, t\sin\theta) + (-s\sin\theta, s\cos\theta), \text{for s} \in \mathbb{R} \tag{3.5}$$

Each t and θ uniquely determine a line in the plane, which means that now we can represent any line in terms of these two parameters. We notice that $\ell_{t,\theta+2\pi} = \ell_{t,\theta}$ and $\ell_{t,\theta+\pi} = \ell_{-t,\theta}$ for all t, θ. This tells us that for $\theta \in [\pi, 2\pi)$ we will get the same lines that we have already got for $\theta \in [0, \pi)$, where the only difference is the opposite sign of $\hat{\boldsymbol{\omega}}$ vector. Therefore, it is sufficient to choose only one of those lines—we can limit ourselves to $\theta \in [0, \pi)$. Note that we can either describe our lines in the terms of the pair θ, t or $\boldsymbol{\omega}, t$. Throughout the thesis we will use both of them, depending on which one suits us better in the given situation.

Example 3.1.1 (*Parametrization in the terms of angle θ and affine parameter t*)**.** Consider a line in Cartesian coordinates given by the equation $y = 1$. From equation (3.1) we get:

$$a = 0, b = 1, c = 1$$

Let us now find our vectors $\boldsymbol{\omega}$ and $\hat{\boldsymbol{\omega}}$:

$$\boldsymbol{\omega} = (0, 1) = (\cos\theta, \sin\theta)$$

Considering that $\theta \in [0, \pi)$, we get $\theta = \pi/2$. Further on, we get: $\hat{\boldsymbol{\omega}} = (-1, 0)$ and $t = 1$ Now we can write our parametrized line as:

$$\ell_{t,\theta} = (0, 1) + (-s, 0), s \in \mathbb{R}$$

If we represent this graphically, it is clear that our obtained line is exactly the same as the initial one $y = 1$, shown in Figure 3.2.

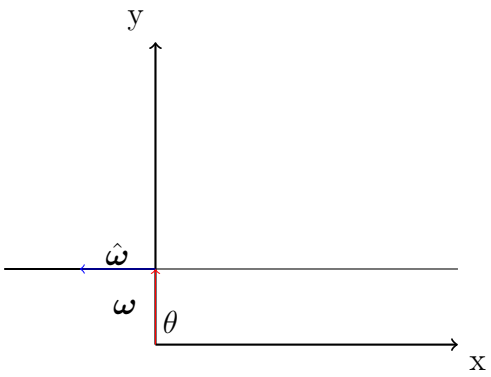

Figure 3.2: Representation of parametrized line $\ell_{1,\pi/2}$

3.2 Line integral of a scalar-valued function

Before we start talking about the Radon transform and its inverse, we have to define a *line integral* which is a necessary tool for the abovementioned transformations.
In general, we can think of line integral as a one-variable function integral over an interval, except that we do not integrate over an interval but over a curve [15]. Suppose we have a function $r(t)$ that represents a parametrisation of a curve, where $t \in [a, b]$ and $a, b \in \mathbb{R}$. Firstly, we will introduce a necessary term that will be used—*arclength* of a parametrised curve.

Arclength of the parametrised curve Since calculating the length of a curve is slightly more complicated than calculating the length of a straight line, we will assume our curve is made up of a series of straight line segments, which we can put together to acquire the desired arclength. We are going to split the interval $[a, b]$ into n equal subintervals $[t_0, t_1]$, $[t_1, t_2]$, $\ldots$, $[t_{n-1}, t_n]$, such that $a = t_0 < t_1 < t_2 < \cdots < t_n = b$.

Further, we say that the length of every subinterval is:

$$\Delta t_i = t_i - t_{i-1} \tag{3.6}$$
$$i \in \{1, 2, 3, \ldots, n\}$$

Obviously, as we increase the number of line segments n, the length of subintervals Δt decreases, and our curve approximation gets more accurate[1].
The length of i-th line segment of a curve is $\|r(t_i) - r(t_{i-1})\|$, because the i-th line segment can be observed as a vector that goes from point $r(t_i)$ to $r(t_{i-1})$. To get the total arclength $\hat{\mathcal{L}}$, we add up all of the segments, which gives us:

$$\hat{\mathcal{L}}(r(t), n) = \sum_{i=1}^{n} \|r(t_i) - r(t_{i-1})\| \tag{3.7}$$

Using (3.6) we get:

$$\hat{\mathcal{L}}(r(t), n) = \sum_{i=1}^{n} \|r(t_i + \Delta t_i) - r(t_{i-1})\| = \sum_{i=1}^{n} \| \frac{r(t_{i-1} + \Delta t_i) - r(t_{i-1})}{\Delta t_i} \| \cdot \Delta t_i \tag{3.8}$$

Using the definition of derivative and Riemann sum for an integral, as $n \to \infty$ in (3.8), we have:

$$\mathcal{L}(r(t)) = \lim_{n \to \infty} \hat{\mathcal{L}}(r(t), n) \tag{3.9}$$

which yields

$$\mathcal{L}(r(t)) = \int_a^b \|r'(t)\| \, \mathrm{d}t. \tag{3.10}$$

Line integral over parametrised curve To take an integral of a scalar-valued function f over a parametrized curve $r(t)$ means to sum up the values at every point of this function and multiply it by the arc length of the curve. For example, we have a spring and we want to compute its mass [15]. Values of the function $f(r(t))$ would, in this case, represent the density of the spring, so its mass at some point would be computed as a product of the density and the curve length "at that point". Accordingly, to find the whole mass of the spring would mean to sum up masses at "all of its points".
Using the same principle as above, we say that the length of i-th line segment is $\|r(t_i) - r(t_{i-1})\|$ and the density of this line segment is $f(r(t_i))$. Previously mentioned mass of the spring

[1] Provided that the curve is sufficiently "well-behaved". We will not go into details here, for more details, see the book [1].

would in that case be written as:

$$\mathcal{M}(r(t), n) = \sum_{i=1}^{n} f(r(t_i))\|r(t_i) - r(t_{i-1})\| \tag{3.11}$$

and the mass of the spring curve that is given parametrically by $r(t)$, $t \in [a, b]$ is given by

$$\lim_{n\to\infty} \mathcal{M}(r(t), n) = \int_a^b f(r(t))\|r'(t)\| \,\mathrm{d}t$$

Thus, we get the following definition of the line integral.

Definition 3.2.1 (*Line integral*)**.** For some scalar function $f : U \to \mathbb{R}$, $U \subseteq \mathbb{R}^n$ the line integral along a smooth curve $\mathcal{C} \subseteq U$ is defined as:

$$\int_{\mathcal{C}} f \,\mathrm{d}s = \int_a^b f(r(t))\|r'(t)\| \,\mathrm{d}t$$

where $r : [a, b] \to \mathcal{C}$ is a parametrization of the curve $\mathcal{C}$, such that $r(a)$ and $r(b)$ are the endpoints of $\mathcal{C}$ and $a < b$.

Example 3.2.2 (*Line integral of a function along the circle*)**.**
Let us find an integral $\int_{\mathcal{C}} \sqrt{x^2 + y^2} \,\mathrm{d}s$, if $\mathcal{C}$ is a circle with center $(\frac{1}{2}, 0)$ and radius $\frac{1}{2}$.
We will firstly find the parametrisation of the given line, then we are going to compute the arc length of the circle. After that, we can easily compute the line integral.

$$\begin{aligned}
r(t) &= (\frac{1}{2} + \frac{1}{2}\cos t, \frac{1}{2}\sin t) \\
r'(t) &= (-\frac{1}{2}\sin t, \frac{1}{2}\cos t) \\
\|r'(t)\| &= \sqrt{\frac{1}{4}\sin^2 t + \frac{1}{4}\cos^2 t} = \frac{1}{2} \\
\int_{\mathcal{C}} \sqrt{x^2 + y^2} \,\mathrm{d}s &= \int_0^{2\pi} \sqrt{(\frac{1}{2} + \frac{1}{2}\cos^2 t) + (\frac{1}{2}\sin^2 t)}\frac{1}{2} \,\mathrm{d}t = \frac{1}{2}
\end{aligned}$$

In the conclusion of this chapter, it is important to mention that line integral does not depend on the parametrisation of the curve, i.e., whatever parametrisation we choose, the value of the integral remains the same.

Chapter 4

The Radon transform

The main theoretical tool of CT is an integral transform discovered by Johann Radon in 1917. Radon proved that one can reconstruct a function defined on a region of a plane by knowing "sufficiently many" integrals along the lines of this function. In this chapter, we state the definition of the transform in Section 4.1 and, at its end, we will briefly indicate the problem of inverting the Radon transform.

4.1 The Radon transform

When we say that f is a function with *bounded support*, we say that its value is zero anywhere outside of some bounded area. If we have a body whose CT scan we want to measure, that body represents the bounded area and the attenuation coefficients within it have non-zero values, whereas the attenuation coefficients outside of the body are considered to be zero. As we have already concluded, the equation of our interest is the Beer's law (2.15). We want to solve this equation in order to find out what the value of $a(s)$ is, and we are going to need the definition of the Radon transform to do so.

Definition 4.1.1 (*The Radon transform* [9])**.** Suppose that f is a function defined in the plane, which, for simplicity, we assume is continuous with bounded support. The integral of f along the line $\ell_{t,\boldsymbol{\omega}}$ is denoted by[1]

$$\mathscr{R}f(t,\boldsymbol{\omega}) = \int_{\ell_{t,\boldsymbol{\omega}}} f \, \mathrm{d}s \tag{4.1}$$

The Radon transform is the collection of line integrals of function f, that are described in parametrised form in terms of affine parameter t and angle θ (See Chapter 3).

Let us now say something about some important properties of the Radon transform [9].

[1] Recall the notation of Section 3.1

Proposition 4.1.2. The following three conditions hold:

1. $$\mathscr{R}(af + bg) = a\mathscr{R}f + b\mathscr{R}g$$

2. $$\mathscr{R}f(t, \boldsymbol{\omega}) = \mathscr{R}f(-t, -\boldsymbol{\omega})$$

   .

3. $$\mathscr{R}f(t, \theta) = \int_{-\infty}^{\infty} f(t\cos\theta - s\sin\theta, t\sin\theta + s\cos\theta)\,\mathrm{d}s$$

for $a, b \in \mathbb{R}$, f, g in the domain of the Radon transform, and $s \in \mathbb{R}$.

Proof. (See the book [9]).

1. Line integral is linear, hence so is the Radon transform:

$$\int_{\ell_{t,\boldsymbol{\omega}}} (af + bg)\,\mathrm{d}s = a\int_{\ell_{t,\boldsymbol{\omega}}} f\,\mathrm{d}s + b\int_{\ell_{t,\boldsymbol{\omega}}} g\,\mathrm{d}s.$$

2. We know that

$$(-\boldsymbol{\omega}) = (-\cos\theta, -\sin\theta)(-\hat{\boldsymbol{\omega}}) = (\sin\theta, -\cos\theta) = -(-\sin\theta, \cos\theta)$$

   which yields

$$\ell_{-t,-\boldsymbol{\omega}} = \{(-t)(-\boldsymbol{\omega}) + s(-\hat{\boldsymbol{\omega}}) = t\boldsymbol{\omega} + (-s)\hat{\boldsymbol{\omega}} : s \in \mathbb{R}\} = \ell_{t,\boldsymbol{\omega}}.$$

3. This follows directly from the representation of parametrised line that we have derived in Chapter 3.

■

Throughout the rest of the thesis, we will mostly use the Radon transform written in the form stated in Property 3, so we will briefly explain the practical meaning of it. The values of θ and t are predefined, while the variable s gets integrated over. For a fixed value of θ, our CT scanner sends a family of parallel X-ray beams that we observe as different lines, each of them having its own different value of t. We can describe this as a cutting the two-dimensional object to slices; one slice is obtained for one fixed angle θ and many different afinne parameters t. This process is repeated, giving us many different *slices* which are "merged together" to produce the initial two-dimensional object.

The process of "merging" the slices actually represents the reconstruction of the object whereas the slices are denoted as the *Radon transform* or sometimes as *projections*. For a better understanding of this idea, look at Figure 4.1. In this figure, where we can think of

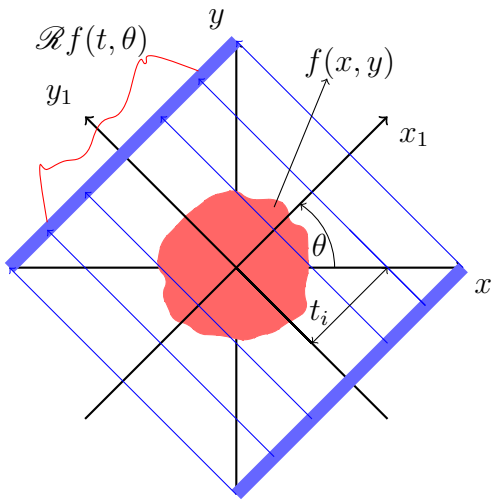

Figure 4.1: The projection/slice for a fixed angle θ

the red object in the middle as the tumor and observe how parallel X-ray beams make the one *projection*(*slice*) for a fixed angle of θ. The projection is represented by red color in the upper left-hand corner of the image. In medical examination, both two-dimensional and three-dimensional scans are used. The real-life equivalent to the Figure 4.1 is shown in Figure 4.3 whereas the real example of a three-dimensional CT scan is shown in Figure 4.2.

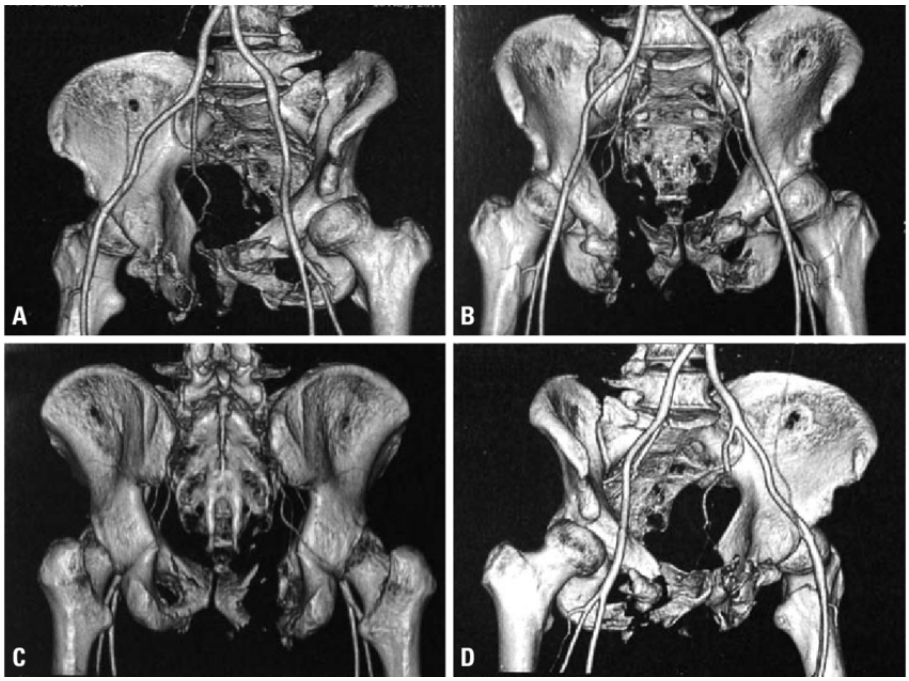

Figure 4.2: Real example of 3D CT scan [3]

Figure 4.3: Real example of 2D CT scan [3]

On the other hand, if we look at the definition of the Radon transform (4.1), on the right-hand side, we have an integral of the function f along multiple lines $\ell_{t,\boldsymbol{\omega}}$, and on the left-hand side, we have the Radon transform. Our function of interest f is the attenuation coefficient $a(s)$. This means that the Radon transform represents the known, measured intensities [5], more precisely $\ln(\frac{i_f}{i_0})$.
Only now it does get completely clear why our initial goal was to find the inverse of the Radon transform. The Radon transform of $a(s)$ is known, while the function f (that is, in our case $a(s)$) on the right-hand side of equation (4.1) is unknown. What gives us the desired function $a(s)$ is exactly the inversion of the Radon transform.

We can conclude that the Radon transform $f \mapsto \mathscr{R}f$ is linear in f, as proved in Section 4.1. However, the linear spaces, where f and $\mathscr{R}f$ live, have infinite dimensions. Thus, one has to apply more subtle methods than just linear algebra to find the inverse of the mapping $f \mapsto \mathscr{R}f$. In particular, one has to be quite precise in defining the linear spaces to where f and $\mathscr{R}f$ belong. Under these conditions, the inverse indeed exists, but its derivation is not straightforward, and it requires an explanation of a few more things. The so-called *Central slice theorem* is one of the techniques for a function reconstruction, and to prove it, we will require a Fourier analysis, which will be explored in-depth in the following chapter.

Chapter 5

Fourier analysis

Joseph Fourier was a French mathematician who found something that would become one of the most fundamental ideas in mathematics. While he was working on the heat equation, he showed that every signal can be represented as a sum of certain sines and cosines and had represented this idea in his work *The Analytical Theory of Heat* from 1822 [11]. For example, if we have some musical wave, we can decompose it into its high and low notes (frequencies). The other example would be radio signals in which we often encounter some noise. This noise represents high frequencies that we wish to eliminate, which is much easier to do when the signal is decomposed into multiple frequencies. To begin our exploration of the Fourier analysis, we will start with the Fourier series, which is where Fourier himself began. Further on, we will show how the idea of the Fourier series can be extended to a more general case—the Fourier transform and its inverse and how these two are related to each other. The last-mentioned fact is of particular significance to us because we exploit the relationship between the two to recover the initial function, shown in the known *Inversion Theorem*, discussed in Section 5.4.

5.1 Fourier Series

Before we start talking about the definition of the Fourier series, let us recall some basic facts and interpretations of the complex exponential function since it makes computations simpler and more clear. The inspiration for this chapter that concerns the Fourier series and Fourier transform (with its properties) is mainly found in books [21],[10] and [13].

The complex exponential function The relationship between the sine, cosine and the exponential function is given by the *Euler's formula* [10]:

$$e^{i\theta} = \cos\theta + i\sin\theta \tag{5.1}$$

From the above-given formula, it is clear that the number $e^{i\theta} \in \mathbb{C}$ represents a point in the plane that can be described by polar coordinates r (in this case, $r = 1$) and θ, so we can think of $t \mapsto e^{i\theta t}$ as of a rotating vector. For example, $e^{2\pi it}$ is a vector rotating around a unit circle, with a frequency of one cycle per second in a counter-clockwise direction. Similarly, $e^{-2\pi it}$ rotates with the same frequency only in the opposite direction. A vector described by $e^{2\cdot 2\pi it}$ rotates at the rate of two cycles per second, so it makes two rotations around a full circle for one second as it needs to cover a distance of 4π in one second. By multiplying our vector with some constant $c \in \mathbb{C}$, we obtain different initial magnitude and direction of our rotating vector. For example, the vector given by $2e^{2\pi it}$ is going to rotate around the circle with radius of 2 instead of radius of 1 as in the previous case. If we want our vector to start rotating from the angle of 30°, we would multiply it by $e^{(\pi/6)i}$.

Fourier series

Definition 5.1.1 (*The Fourier series*)**.** Every continuous, periodic function f with the period of T can be expressed as follows:

$$f(t) = \sum_{n=-\infty}^{\infty} c_n e^{\frac{i2\pi n}{T}t} \tag{5.2}$$

where $n \in \mathbb{Z}$ and the coefficient c_n is given by

$$c_n = \frac{1}{T}\int_{-T/2}^{T/2} f(t)e^{-\frac{i2\pi n}{T}t}\,\mathrm{d}t \tag{5.3}$$

Let us explain the above formulas rather intuitively. We can think of our function $f(t)$ as a sum of different rotating vectors. To get a good approximation of the function, we need to find corresponding coefficients c_n. Consider, for example, a constant term c_0. To find c_0, we are integrating our function over the period, which we then divide by the length of that period. This process is nothing but taking an average value of the function:

$$c_0 = \frac{1}{T}\int_{-T/2}^{T/2} f(t)\,\mathrm{d}t = \frac{1}{T}\int_{-T/2}^{T/2} (\dots c_{-1}e^{-\frac{i2\pi\cdot(-1)}{T}t} + c_0 e^{-\frac{i2\pi\cdot 0}{T}t} + c_1 e^{-\frac{i2\pi\cdot 1}{T}t}\dots)\,\mathrm{d}t \tag{5.4}$$

The reason for getting exactly the c_0 in this process is that the only "steady" vector is the one that corresponds to the coefficient c_0, and at the same time, it is the only one that has a non-zero average value since the average value of all the rotating vectors in the sum in equation (5.4) is going to be zero. Every other coefficient is obtained in the same way—exactly this is where the element $e^{-\frac{i2\pi n}{T}}$ comes into play. For example, if we wish to get c_3, we can do so by multiplying a function with the term $e^{-\frac{i2\pi\cdot 3}{T}}$, which makes our

desired vector "stationary" rather than rotating, and then taking its average value.

5.2 Fourier transform

Now when we know and understand the basic principle of the Fourier series, we can extend the same idea to the functions that are not necessarily periodic. First of all, we want to derive an equivalent to the Fourier series for the non-periodic functions. After that, we will provide an official definition with some important properties of the Fourier transform. Let us rewrite our equations (5.2) and (5.3) in the following manner. We put

$$\alpha_n = \frac{2\pi n}{T}$$

$$h(\alpha_n) = \frac{T}{2\pi} c_n$$

which yields

$$h(\alpha_n) = \frac{1}{2\pi} \int_{-T/2}^{T/2} f(t) e^{-it\alpha_n} \, \mathrm{d}t \tag{5.5}$$

$$f(t) = \sum_{n=-\infty}^{\infty} h(\alpha_n) e^{it\alpha_n} \frac{2\pi}{T} = \sum_{n=-\infty}^{\infty} h(\alpha_n) e^{it\alpha_n} (\alpha_n - \alpha_{n-1}) = \sum_{n=-\infty}^{\infty} h(\alpha_n) e^{it\alpha_n} \Delta\alpha_n \tag{5.6}$$

In equation (5.6) we have used the fact that:

$$\frac{2\pi}{T} = \frac{2\pi n}{T} - \frac{2\pi(n-1)}{T} = \alpha_n - \alpha_{n-1}$$

As $T \to \infty$ then $\Delta\alpha_n \to 0$, and we get

$$h(\alpha) = \frac{1}{2\pi} \int_{-\infty}^{\infty} f(t) e^{-it\alpha} \, \mathrm{d}t \tag{5.7}$$

$$f(t) = \int_{-\infty}^{\infty} h(\alpha) e^{it\alpha} \, \mathrm{d}\alpha \tag{5.8}$$

The formula (5.7) is known as the *Fourier transform*, whereas (5.8) is the *Fourier inversion formula*. We can now see the equivalence between the Fourier series and Fourier transform; the Fourier transform formula is equivalent to the coefficient formula (5.3), and the inverse Fourier transform is equivalent to the Fourier series decomposition (5.2).
While deriving the above formulas, we have not indicated any requirements that f must meet in order for them to be valid. Even though we are not going to go into a detailed explanation of this, let us mention a few key points.

The precise description of the class of functions to which the Fourier transform can be applied is not easy. A common "space" of functions that one meets in the literature is the so-called *Schwartz space*.

Remark 5.2.1 (The Schwartz space $\mathcal{S}$)**.** A function $f(\boldsymbol{x}) = f(x_1, x_2 \dots x_n)$ belongs to the Schwartz space $\mathcal{S}(\mathbb{R}^n)$ if all its partial derivatives are rapidly decreasing. By saying rapidly decreasing, we mean that by multiplying the function $f(x)$ by any polynomial $p(x)$, as $x \to \infty$, $p(x)f(x)$ will go to zero. This property is important because whenever a function f belongs to the Schwartz space, its Fourier transform belongs to the Schwartz space too. Hence, in order to talk about the Fourier transform of the function, we need to ensure that it belongs to the Schwartz space. Although the functions that we meet in practice of CT often do not belong to $\mathcal{S}(\mathbb{R}^n)$, there are methods to overcome this problem. We will not go into technical details here, for more information on this topic, see the book [21].

5.3 Fourier transform in n dimensions and its properties

Definition 5.3.1 (*The Fourier transform and its inverse*)**.** For a given function $f \in \mathcal{S}(\mathbb{R}^n)$, the Fourier transform of f is defined as:

$$\{\mathcal{F}f(\boldsymbol{t})\} = \frac{1}{(2\pi)^{\frac{n}{2}}} \int_{\mathbb{R}^n} f(\boldsymbol{t}) e^{-i\langle \boldsymbol{t}, \boldsymbol{\alpha} \rangle} \, \mathrm{d}\boldsymbol{t} = \hat{f}(\boldsymbol{\alpha}) \tag{5.9}$$

where $\mathcal{F}f(\boldsymbol{t})$ represents the Fourier transform of the function $f(\boldsymbol{t})$, which will more often be denoted as $\hat{f}(\boldsymbol{\alpha})$, since the variable $\boldsymbol{t}$ gets integrated out, so the new function is a function that depends only on $\boldsymbol{\alpha}$. The inverse Fourier transform of f is defined as:

$$\{\mathcal{F}^{-1}f(\boldsymbol{\alpha})\} = \frac{1}{(2\pi)^{\frac{n}{2}}} \int_{\mathbb{R}^n} f(\boldsymbol{\alpha}) e^{i\langle \boldsymbol{t}, \boldsymbol{\alpha} \rangle} \, \mathrm{d}\boldsymbol{\alpha} = \check{f}(\boldsymbol{t}) \tag{5.10}$$

Remark 5.3.2. One may ask, what exactly is the reason for putting a minus in the exponent in the Fourier transform and the plus sign in the inversion. The truth is—it is just a convention. If we recall our explanation of the complex exponential in the term of rotating vectors, the sign only represents the direction of the rotation (and minus is, by convention, a counter-clockwise direction). Another question one may ask is, why have we put the $(\frac{1}{2\pi})^{\frac{n}{2}}$ with both formulas, since in some literature it can be found written differently. The answer is that it is up to our choice if we are going to put the $(\frac{1}{2\pi})^n$ with the inverse or split it so that we have $(\frac{1}{2\pi})^{\frac{n}{2}}$ along with both formulas, or we can even put it in the exponential so we would not have any factor that multiplies the integral.

Let us now say something about several properties of the Fourier transform. We will show their validity in general case (for n dimensions), although we will be using only one and two dimensions in the further work.

Theorem 5.3.3 (Properties of the Fourier transform)**.** For all the properties that follow, we assume that both functions $f \in \mathcal{S}(\mathbb{R}^n)$ and $g \in \mathcal{S}(\mathbb{R}^n)$ and $\boldsymbol{t}, \boldsymbol{\alpha}, \boldsymbol{m} \in \mathbb{R}^n$.

1. Additivity
$$\mathcal{F}\{(f+g)(\boldsymbol{t})\} = \mathcal{F}\{f(\boldsymbol{t})\} + \mathcal{F}\{g(\boldsymbol{t})\}$$

2. Constant multiples
$$\mathcal{F}\{cf(\boldsymbol{t})\} = c\mathcal{F}\{f(\boldsymbol{t})\}$$
for $c \in \mathbb{R}$.

3. Linearity
$$\mathcal{F}\{(af+bg)(\boldsymbol{t})\} = a\mathcal{F}\{f(\boldsymbol{t})\} + b\mathcal{F}\{g(\boldsymbol{t})\}$$
for $a, b \in \mathbb{R}$.

4. Shifting—Translation
$$\mathcal{F}\{f(\boldsymbol{t}-\boldsymbol{m})\} = e^{-i\langle\boldsymbol{\alpha},\boldsymbol{m}\rangle}\hat{f}(\boldsymbol{\alpha})$$

5. Shifting—Modulation
$$\mathcal{F}\{e^{i\langle\boldsymbol{\alpha},\boldsymbol{m}\rangle}f(\boldsymbol{t})\} = \hat{f}(\boldsymbol{\alpha}-\boldsymbol{m})$$

6. Scaling
$$\mathcal{F}\{f(k\boldsymbol{t})\} = \frac{1}{|a|}\hat{f}(\frac{\boldsymbol{\alpha}}{k})$$
for $k \in \mathbb{R} \setminus \{0\}$.

Proof. 1. Additivity

$$\begin{aligned}\mathcal{F}\{(f+g)(\boldsymbol{t})\} = \int_{\mathbb{R}^n}(f(\boldsymbol{t})+g(\boldsymbol{t}))e^{-i\langle\boldsymbol{t},\boldsymbol{\alpha}\rangle}\,\mathrm{d}\boldsymbol{t} &= \int_{\mathbb{R}^n}f(\boldsymbol{t})e^{-i\langle\boldsymbol{t},\boldsymbol{\alpha}\rangle}\,\mathrm{d}\boldsymbol{t} + \int_{\mathbb{R}^n}g(\boldsymbol{t})e^{-i\langle\boldsymbol{t},\boldsymbol{\alpha}\rangle}\,\mathrm{d}\boldsymbol{t}\\ &= \mathcal{F}\{f(\boldsymbol{t})\} + \mathcal{F}\{g(\boldsymbol{t})\}\end{aligned}$$

2. Constant multiplies

$$\mathcal{F}\{cf(\boldsymbol{t})\} = c\int_{\mathbb{R}^n}f(\boldsymbol{t})e^{-i\langle\boldsymbol{t},\boldsymbol{\alpha}\rangle}\,\mathrm{d}\boldsymbol{t} = c\mathcal{F}\{f(\boldsymbol{t})\}$$

for $c \in \mathbb{R}$.

3. Linearity follows from properties 1 and 2.

4. Shifting—Translation

$$\mathcal{F}\{f(\boldsymbol{t}-\boldsymbol{m})\} = \int_{\mathbb{R}^n} f(\boldsymbol{t}-\boldsymbol{m}) e^{-i\langle \boldsymbol{t},\boldsymbol{\alpha}\rangle}\,\mathrm{d}\boldsymbol{t} = e^{-i\langle \boldsymbol{\alpha},\boldsymbol{m}\rangle}\hat{f}(\boldsymbol{\alpha})$$

We can make a simple substitution:

$$\begin{aligned} \boldsymbol{t}-\boldsymbol{m} &= \boldsymbol{u} \\ \mathrm{d}\boldsymbol{t} &= \mathrm{d}\boldsymbol{u} \\ \boldsymbol{u}+\boldsymbol{m} &= \boldsymbol{t} \end{aligned}$$

Further, we obtain

$$\int_{\mathbb{R}^n} f(\boldsymbol{u}) e^{-i\langle \boldsymbol{\alpha},\boldsymbol{u}+\boldsymbol{m}\rangle}\,\mathrm{d}\boldsymbol{u} = e^{-i\langle \boldsymbol{\alpha},\boldsymbol{m}\rangle}\int_{\mathbb{R}^n} f(\boldsymbol{u}) e^{-i\langle \boldsymbol{u},\boldsymbol{\alpha}\rangle}\,\mathrm{d}\boldsymbol{t} = e^{-i\langle \boldsymbol{\alpha},\boldsymbol{m}\rangle}\hat{f}(\boldsymbol{\alpha})$$

5. Shifting—Modulation

$$\mathcal{F}\{e^{i\langle \boldsymbol{\alpha},\boldsymbol{m}\rangle} f(\boldsymbol{t})\} = \int_{\mathbb{R}^n} e^{i\langle \boldsymbol{\alpha},\boldsymbol{m}\rangle} g(\boldsymbol{t}) e^{-i\langle \boldsymbol{\alpha},\boldsymbol{t}\rangle}\,\mathrm{d}\boldsymbol{t} = \int_{\mathbb{R}^n} f(\boldsymbol{t}) e^{-i\langle \boldsymbol{t},(\boldsymbol{\alpha}-\boldsymbol{m})\rangle}\,\mathrm{d}\boldsymbol{t} = \hat{f}(\boldsymbol{\alpha}-\boldsymbol{m})$$

6. Scaling

For $k > 0$:

$$\mathcal{F}\{f(k\boldsymbol{t})\} = \int_{\mathbb{R}^n} f(k\boldsymbol{t}) e^{-i\langle \boldsymbol{t},\boldsymbol{\alpha}\rangle}\,\mathrm{d}\boldsymbol{t}$$

Again, we make a substitution:

$$\begin{aligned} \boldsymbol{u} &= k\boldsymbol{t} \\ \boldsymbol{t} &= \frac{\boldsymbol{u}}{k} \\ \mathrm{d}\boldsymbol{u} &= k\,\mathrm{d}\boldsymbol{t} \end{aligned}$$

We get

$$\frac{1}{k}\int_{\mathbb{R}^n} f(k\boldsymbol{u}) e^{-\frac{i\langle \boldsymbol{u},\boldsymbol{\alpha}\rangle}{k}}\,\mathrm{d}\boldsymbol{t} = \frac{1}{k}\hat{f}(\frac{\boldsymbol{\alpha}}{k})$$

Similarly, for $k < 0$, we would get the same result with the opposite sign, which is why the general result is written using an absolute value.

■

5.4 The inversion theorem

Generally, loads of different approaches to the proof of this theorem can be found in the literature. Before proving the theorem itself, we need to say something about the *Dirac delta function*, which is not actually a function in the way of the mathematical definition of the function, but a distribution. Nonetheless, it is frequently referred to as a function, but we will not go into the distributions in-depth here. More information about the distributions and their properties can be found, for example, in Appendix B of the book [7]. For the *Inversion theorem* proof, we mainly refer to [19].

The Dirac Delta function Suppose we need a function $\delta : \mathbb{R}^n \to \mathbb{R}$ that satisfies the following two properties:

1. $\delta(\boldsymbol{t}) = 0$ for all $\boldsymbol{t} \neq \boldsymbol{0}$
2. $\int_{\mathbb{R}^n} \delta(\boldsymbol{t}) \mathrm{d}\boldsymbol{t} = 1$

Clearly, no such function can exist in reality, but we can seek to approximate δ by a sequence of functions $\{\delta_k(\boldsymbol{t})\}_{k=1}^{\infty}$ with the following properties:

(1.1)
$$\int_{\mathbb{R}^n} \delta_k(\boldsymbol{t}) \mathrm{d}\boldsymbol{t} = 1 \text{ for all } k \geq 1$$

(1.2) There exists M such that for all $k \geq 1$
$$\int_{\mathbb{R}^n} |\delta_k(\boldsymbol{t})| \mathrm{d}\boldsymbol{t} \leq M$$

(1.3) For all $K > 0$ we have
$$\lim_{k\to\infty} \int_{\{\boldsymbol{t} | \|\boldsymbol{t}\| \geq K\}} |\delta_k(\boldsymbol{t})| \, \mathrm{d}\boldsymbol{t} = 0$$
where we define $\|\boldsymbol{t}\| = \max\limits_{i=1,\ldots,n} |t_i|$

Proposition 5.4.1. Let us choose the approximation of our function δ as follows:
$$\delta_k(\boldsymbol{t}) = \delta_k(t_1, t_2, \ldots, t_n) = \frac{\frac{k}{\pi}}{1 + (kt_1)^2} \cdot \frac{\frac{k}{\pi}}{1 + (kt_2)^2} \cdot \ldots \frac{\frac{k}{\pi}}{1 + (kt_n)^2}$$
for $k \geq 1$. First of all, we need to show that properties (1.1)-(1.3) are indeed fulfilled.

Proof. (1.1)
$$\int_{\mathbb{R}^n} \delta_k(\boldsymbol{t}) \mathrm{d}\boldsymbol{t} = \int_{\mathbb{R}} \cdots \int_{\mathbb{R}} \frac{\frac{k}{\pi}}{1 + (kt_1)^2} \cdot \ldots \cdot \frac{\frac{k}{\pi}}{1 + (kt_n)^2} \, \mathrm{d}t_n \ldots \mathrm{d}t_1$$

By making a substitution, we get

$$kt_i = u_i$$

$$k\,\mathrm{d}t_i = \mathrm{d}u_i$$

for $i = 1, 2, \ldots, n$, which gives us

$$\int_{\mathbb{R}} \cdots \int_{\mathbb{R}} \frac{\frac{1}{\pi}}{1+u_1^2} \cdots \frac{\frac{1}{\pi}}{1+u_n^2}\,\mathrm{d}u_n \ldots \mathrm{d}u_1 = \frac{1}{\pi}\left[\lim_{u\to\infty} \arctan(u) - \lim_{u\to-\infty} \arctan(u)\right]^n = \left(\frac{\pi}{\pi}\right)^n = 1$$

(1.2) By (1.1), we know that the value of the integral is 1, so choose, for example, $M = 2$.

(1.3) We want to compute

$$\lim_{k\to\infty} \int_{\{\boldsymbol{t}\,|\,\|\boldsymbol{t}\|\geq K\}} \delta_k(\boldsymbol{t})\,\mathrm{d}\boldsymbol{t} = \lim_{k\to\infty} \int_{\{\boldsymbol{t}\,|\,\|\boldsymbol{t}\|\geq K\}} \frac{\frac{k}{\pi}}{1+(kt_1)^2} \cdot \cdots \cdot \frac{\frac{k}{\pi}}{1+(kt_n)^2}\,\mathrm{d}t_n \ldots \mathrm{d}t_1$$

As in previous case, we can make a substitution:

$$kt_i = u_i$$

$$\mathrm{d}t_i = \mathrm{d}u_i$$

Additionaly, we say that:

$$A_i = \{ \begin{pmatrix} a_1 \\ a_2 \\ \vdots \\ a_n \end{pmatrix} \mid |a_i| \geq K \}$$

which yields

$$\bigcup_{i=1}^{n} A_i = \{ \begin{pmatrix} a_1 \\ a_2 \\ \vdots \\ a_n \end{pmatrix} \mid \max_{i=1,\ldots,n} |a_i| \geq K \}$$

We get

$$\begin{aligned}0 &\leq \int_{\bigcup_{i=1}^{n} A_i} \frac{1}{1+u_1^2}\cdots\frac{1}{1+u_n^2}\,\mathrm{d}a_n\ldots\mathrm{d}a_1 \leq \sum_{i=1}^{n}\int_{A_i}\frac{1}{1+u_1^2}\cdots\frac{1}{1+u_n^2}\,\mathrm{d}a_n\ldots\mathrm{d}a_1\\ &= \sum_{i=1}^{n}\Big((2\int_{\{a_i||a_i|\geq K\}}\frac{1}{1+a_i^2}\,\mathrm{d}a_i)\int_{-\infty}^{\infty}\cdots\int_{-\infty}^{\infty}\prod_{j\neq i}\frac{1}{1+a_j^2}\,\mathrm{d}a_j\ldots\mathrm{d}a_n\Big)\\ &= \pi^{n-1}\sum_{i=1}^{n}2\int_{K}^{\infty}\frac{1}{1+a_i^2}\,\mathrm{d}a_i = 2\cdot n\cdot\pi^{n-1}(\frac{\pi}{2}-\arctan K)\xrightarrow{K\to\infty}0.\end{aligned}$$

■

Remark 5.4.2. In the above proof, we have used the fact that for any $f \geq 0$ we have:

$$\int_{\bigcup_{i=1}^{n} A_i} f \leq \sum_{i=1}^{n}\int_{A_i} f$$

We can additionally observe that, for every $K > 0$ and every $\{\boldsymbol{t} \mid \|\boldsymbol{t}\| \geq K\}$ and every $k \geq 1$ we have

$$\begin{aligned}\delta_k(\boldsymbol{t}) = \frac{\frac{k}{\pi}}{1+(kt_1)^2}\cdot\ldots\cdot\frac{\frac{k}{\pi}}{1+(kt_n)^2} &= (\frac{1}{k})^n\frac{\frac{k^2}{\pi}}{1+(kt_1)^2}\cdot\ldots\cdot\frac{\frac{k^2}{\pi}}{1+(kt_n)^2}\\ &\leq (\frac{1}{k})^n\frac{1}{\pi(t_1^2+\cdots+t_n^2)} \leq (\frac{1}{k})^n\frac{1}{\pi K^2}\end{aligned} \tag{5.11}$$

For $\|\boldsymbol{t}\| \geq K$ we can rewrite (5.11) as:

$$|\delta_k(\boldsymbol{t})| \leq B_k\cdot(\frac{1}{k})^n \tag{5.12}$$

where

$$B_k = \frac{1}{\pi K^2}$$

.

Theorem 5.4.3 (*Sifting theorem*)**.** If $h : \mathbb{R}^n \to \mathbb{R}$ is an integrable function, continuous at $\boldsymbol{t} \in \mathbb{R}^n$, and δ_k is our approximation of the Dirac delta function, then

$$\lim_{k\to\infty}\int_{\mathbb{R}^n} h(\boldsymbol{t}-\boldsymbol{\tau})\delta_k(\boldsymbol{\tau})\,\mathrm{d}\boldsymbol{\tau} = h(\boldsymbol{t})$$

Proof. Let us say that

$$e_k = h(\boldsymbol{t}) - \int_{\mathbb{R}^n} h(\boldsymbol{t}-\boldsymbol{\tau})\delta_k(\boldsymbol{\tau})\,\mathrm{d}\boldsymbol{\tau}$$

and observe that

$$h(\boldsymbol{t}) = h(\boldsymbol{t}) \cdot \int_{\mathbb{R}^n} \delta_k(\boldsymbol{\tau})\mathrm{d}\boldsymbol{\tau} = \int_{\mathbb{R}^n} h(\boldsymbol{t})\delta_k(\boldsymbol{\tau})\mathrm{d}\boldsymbol{\tau}$$

Hence,

$$e_k = \int_{\mathbb{R}^n} (h(\boldsymbol{t}) - h(\boldsymbol{t}-\boldsymbol{\tau}))\delta_k(\boldsymbol{\tau})\mathrm{d}\boldsymbol{\tau}$$

Let us now choose $\varepsilon \in \mathbb{R}, \varepsilon > 0$. Since h is continuous at $\boldsymbol{t}$, there exists $K \in \mathbb{R}, K > 0$ such that

$$|h(\boldsymbol{t}) - h(\boldsymbol{t}-\boldsymbol{\tau}))| < \varepsilon$$

for all $\|\boldsymbol{\tau}\| < K$. Thus,

$$\begin{aligned} |e_k| &= |\int_{\mathbb{R}^n} (h(\boldsymbol{t}) - h(\boldsymbol{t}-\boldsymbol{\tau}))\delta_k(\boldsymbol{\tau})\mathrm{d}\boldsymbol{\tau}| \leq \int_{\mathbb{R}^n} |h(\boldsymbol{t}) - h(\boldsymbol{\tau}-\boldsymbol{t})|\delta_k(\boldsymbol{\tau})\mathrm{d}\boldsymbol{\tau} \\ &= \int_{\{\boldsymbol{t}|\|\boldsymbol{t}\|<K\}} |h(\boldsymbol{t}) - h(\boldsymbol{\tau}-\boldsymbol{t})|\delta_k(\boldsymbol{\tau})\,\mathrm{d}\boldsymbol{\tau} + \int_{\{\boldsymbol{t}|\|\boldsymbol{t}\|\geq K\}} |h(\boldsymbol{t}) - h(\boldsymbol{\tau}-\boldsymbol{t})|\delta_k(\boldsymbol{\tau})\,\mathrm{d}\boldsymbol{\tau} \end{aligned}$$

For clarity, we will denote the left-hand side of the last line of the above equation by I_k and the right-hand side by J_k Further on, we have

$$\begin{aligned} I_k &= \int_{\{\boldsymbol{t}|\|\boldsymbol{t}\|<K\}} |h(\boldsymbol{t}) - h(\boldsymbol{\tau}-\boldsymbol{t})|\delta_k(\boldsymbol{\tau})\,\mathrm{d}\boldsymbol{\tau} \leq \varepsilon \int_{\{\boldsymbol{t}|\|\boldsymbol{t}\|<K\}} \delta_k(\boldsymbol{\tau})\,\mathrm{d}\boldsymbol{\tau} \\ &\leq \varepsilon \int_{\mathbb{R}^n} \mathrm{d}\boldsymbol{\tau} \leq \varepsilon M \end{aligned}$$

Where we have used Property (1.2). As for the J_k, we have:

$$\begin{aligned} J_k &= \int_{\{\boldsymbol{t}|\|\boldsymbol{t}\|\geq K\}} |h(\boldsymbol{t}) - h(\boldsymbol{\tau}-\boldsymbol{t})|\delta_k(\boldsymbol{\tau})\,\mathrm{d}\boldsymbol{\tau} \\ &\leq \int_{\{\boldsymbol{t}|\|\boldsymbol{t}\|\geq K\}} |h(\boldsymbol{t})|\delta_k(\boldsymbol{\tau})\,\mathrm{d}\boldsymbol{\tau} - \int_{\{\boldsymbol{t}|\|\boldsymbol{t}\|\geq K\}} |h(\boldsymbol{t}-\boldsymbol{\tau})|\delta_k(\boldsymbol{\tau})\,\mathrm{d}\boldsymbol{\tau} \\ &\leq |h(\boldsymbol{t})| \int_{\{\boldsymbol{t}|\|\boldsymbol{t}\|\geq K\}} \delta_k(\boldsymbol{\tau})\,\mathrm{d}\boldsymbol{\tau} - \frac{B_k}{k^n} \int_{\{\boldsymbol{t}|\|\boldsymbol{t}\|\geq K\}} |h(\boldsymbol{t}-\boldsymbol{\tau})|\,\mathrm{d}\boldsymbol{\tau} \end{aligned}$$

By Property (1.3), the left-hand side of the given equation goes to 0 as k goes to ∞. As for the right-hand side, we can write it as:

$$\frac{B_k}{k^n} \int_{\mathbb{R}^n} |h(\boldsymbol{\tau})|\mathrm{d}\boldsymbol{\tau}$$

which goes to 0 as $k \to \infty$. Hence, we get that $|e_k| \leq I_k + J_k$, with the right-hand side tending to zero. This proves the theorem. ■

Theorem 5.4.4. Suppose h and $\hat{g}$ are integrable functions. We define[1] $\hat{h}(\boldsymbol{\omega})$ as the

[1]Recall the convention mentioned in Remark 5.3.2. For convenience of computations we use the

Fourier transform of h and $g(\boldsymbol{t})$ as an inverse Fourier transform of $\hat{g}$:

$$\hat{h}(\boldsymbol{\omega}) = \frac{1}{(2\pi)^{\frac{n}{2}}} \int_{\mathbb{R}^n} h(\boldsymbol{t}) e^{-i\langle \boldsymbol{\omega}, \boldsymbol{t} \rangle} \mathrm{d}\boldsymbol{t}$$

$$g(\boldsymbol{t}) = \frac{1}{(2\pi)^{\frac{n}{2}}} \int_{\mathbb{R}^n} e^{i\langle \boldsymbol{\omega}, \boldsymbol{t} \rangle} \mathrm{d}\boldsymbol{\omega}$$

Then the following equality holds for all $\boldsymbol{t} \in \mathbb{R}^n$:

$$\int_{\mathbb{R}^n} h(\boldsymbol{t} - \boldsymbol{\tau}) g(\boldsymbol{\tau}) \mathrm{d}\boldsymbol{\tau} = \int_{\mathbb{R}^n} \hat{h}(\boldsymbol{\omega}) e^{i\langle \boldsymbol{\omega}, \boldsymbol{t} \rangle} \mathrm{d}\boldsymbol{\omega}$$

Proof. By changing the variables $\boldsymbol{t} - \boldsymbol{\tau} = \boldsymbol{\theta}$ we get:

$$\int_{\mathbb{R}^n} h(\boldsymbol{t} - \boldsymbol{\tau}) g(\boldsymbol{\tau}) \mathrm{d}\boldsymbol{\tau} = \int_{\mathbb{R}^n} h(\boldsymbol{\theta}) g(\boldsymbol{t} - \boldsymbol{\theta}) \mathrm{d}\boldsymbol{\theta}$$

From the definition of $g(\boldsymbol{t})$, it follows that

$$g(\boldsymbol{t} - \boldsymbol{\theta}) = \frac{1}{(2\pi)^{\frac{n}{2}}} \int_{\mathbb{R}^n} e^{i\langle \boldsymbol{\omega}, (\boldsymbol{t} - \boldsymbol{\theta}) \rangle} \mathrm{d}\boldsymbol{\omega}$$

Furthermore, we have

$$\begin{aligned} \int_{\mathbb{R}^n} h(\boldsymbol{t} - \boldsymbol{\tau}) g(\boldsymbol{\tau}) \mathrm{d}\boldsymbol{\tau} &= \int_{\mathbb{R}^n} h(\boldsymbol{\theta}) \left(\frac{1}{(2\pi)^{\frac{n}{2}}} \int_{\mathbb{R}^n} e^{i\langle \boldsymbol{\omega}, (\boldsymbol{t} - \boldsymbol{\theta}) \rangle} \mathrm{d}\boldsymbol{\omega} \right) \mathrm{d}\boldsymbol{\theta} \\ &= \frac{1}{(2\pi)^{\frac{n}{2}}} \int_{\mathbb{R}^n} \left(\int_{\mathbb{R}^n} h(\boldsymbol{\theta}) e^{-i\langle \boldsymbol{\omega}, \boldsymbol{\theta} \rangle} \mathrm{d}\boldsymbol{\theta} \right) e^{i\langle \boldsymbol{\omega}, \boldsymbol{t} \rangle} \mathrm{d}\boldsymbol{\omega} \end{aligned}$$

From the definition of $\hat{h}(\boldsymbol{\omega})$, we see that middle integral is $(2\pi)^{\frac{n}{2}} \cdot \hat{h}(\boldsymbol{\omega})$ which yields

$$\int_{\mathbb{R}^n} h(\boldsymbol{t} - \boldsymbol{\tau}) g(\boldsymbol{\tau}) \mathrm{d}\boldsymbol{\tau} = \int_{\mathbb{R}^n} \hat{h}(\boldsymbol{\omega}) e^{i\langle \boldsymbol{\omega}, \boldsymbol{t} \rangle} \mathrm{d}\boldsymbol{\omega}$$

which is exactly what we wanted to prove. ∎

Before actually coming to the proof of the inversion theorem, we need one more thing—the Fourier transform of $\delta_k(\boldsymbol{t})$, which will be denoted by $\Delta_k(\boldsymbol{\omega})$.

$$\Delta_k(\boldsymbol{\omega}) = \frac{1}{(2\pi)^{\frac{n}{2}}} \int_{\mathbb{R}^n} \delta_k(\boldsymbol{t}) e^{-i\langle \boldsymbol{\omega}, \boldsymbol{t} \rangle} \mathrm{d}\boldsymbol{t} = \frac{1}{(2\pi)^{\frac{n}{2}}} e^{-\frac{\|\omega\|}{k}}$$

Additionally, we observe that:

$$\lim_{k \to \infty} \Delta_k(\boldsymbol{\omega}) = \frac{1}{(2\pi)^{\frac{n}{2}}} \lim_{k \to \infty} e^{-\frac{\|\omega\|}{k}} = 1.$$

"symmetric" distribution of $\frac{1}{(2\pi)^n}$ here.

Theorem 5.4.5 (*Consequence of Theorem 5.4.4*)**.** For an integrable function $h : \mathbb{R}^n \to \mathbb{R}$, whose Fourier transform is denoted by $\hat{h}(\boldsymbol{\omega})$, we state that

$$h(\boldsymbol{t}) = \lim_{k\to\infty} \frac{1}{(2\pi)^{\frac{n}{2}}} \int_{\mathbb{R}^n} \hat{h}(\boldsymbol{\omega})\Delta_k(\boldsymbol{\omega})e^{i\langle\boldsymbol{\omega},\boldsymbol{t}\rangle}\mathrm{d}\boldsymbol{\omega}$$

Proof. By using Theorem 5.4.4 we have

$$\int_{\mathbb{R}^n} \hat{h}(\boldsymbol{\omega})\Delta_k(\boldsymbol{\omega})e^{i\langle\boldsymbol{\omega},\boldsymbol{t}\rangle}\mathrm{d}\boldsymbol{\omega} = \int_{\mathbb{R}^n} h(\boldsymbol{t}-\boldsymbol{\tau})\delta_k(\boldsymbol{\tau})\mathrm{d}\boldsymbol{\tau}$$

Further on, we can apply *Sifting theorem* 5.4.3 and prove that indeed

$$\lim_{k\to\infty} \int_{\mathbb{R}^n} h(\boldsymbol{t}-\boldsymbol{\tau})\delta_k(\boldsymbol{\tau})\mathrm{d}\boldsymbol{\tau} = h(\boldsymbol{t})$$

. ■

Finally, we have everything we need to prove that by applying the inverse Fourier transform on a Fourier transform of a given function, we actually get our initial function. This is exactly what the Inversion theorem states.

Theorem 5.4.6 (*The inversion theorem*)**.** For an integrable function $h : \mathbb{R}^n \to \mathbb{R}$ whose Fourier transform $\hat{h}$ we define as:

$$\hat{h}(\boldsymbol{\omega}) = \frac{1}{(2\pi)^{\frac{n}{2}}} \int_{\mathbb{R}^n} h(\boldsymbol{t})e^{-i\langle\boldsymbol{\omega},\boldsymbol{t}\rangle}\mathrm{d}\boldsymbol{t}$$

we claim that

$$h(\boldsymbol{t}) = \frac{1}{(2\pi)^{\frac{n}{2}}} \int_{\mathbb{R}^n} \hat{h}(\boldsymbol{\omega})e^{i\langle\boldsymbol{\omega},\boldsymbol{t}\rangle}\mathrm{d}\boldsymbol{\omega}$$

holds for all $\boldsymbol{t} \in \mathbb{R}^n$.

Proof. As we have already concluded in Theorem 5.4.5

$$h(\boldsymbol{t}) = \lim_{k\to\infty} \frac{1}{(2\pi)^{\frac{n}{2}}} \int_{\mathbb{R}^n} \hat{h}(\boldsymbol{\omega})\Delta_k(\boldsymbol{\omega})e^{i\langle\boldsymbol{\omega},\boldsymbol{t}\rangle}\mathrm{d}\boldsymbol{\omega}$$

By using the fact that

$$\lim_{k\to\infty} \Delta_k(\boldsymbol{\omega}) = 1$$

we prove that

$$h(\boldsymbol{t}) = \frac{1}{(2\pi)^{\frac{n}{2}}} \int_{\mathbb{R}^n} \hat{h}(\boldsymbol{\omega})e^{i\langle\boldsymbol{\omega},\boldsymbol{t}\rangle}\mathrm{d}\boldsymbol{\omega}$$

does indeed hold. ■

Chapter 6

Central slice theorem

In this chapter, we have finally arrived at the point where we will apply everything we have learned so far to demonstrate how to complete our desired reconstruction. *The central slice theorem* is a theorem that connects the Radon transform, and the Fourier transform in a way that greatly simplifies our reconstruction procedure, and it is the basis for some other reconstruction methods that are being used in this field. The inspiration for the proof of this theorem can mainly be found in books [5], [13] and [7].

6.1 The proof of the Central slice theorem

Theorem 6.1.1 (*The Central slice theorem*)**.** If f is a function that has defined both the Radon and the Fourier transform, $r \in \mathbb{R}$ and $\theta \in [0, 2\pi)$ then

$$(\mathcal{F}_2 f)(r\cos\theta, r\sin\theta) = \Big(\mathcal{F}_1(\mathscr{R}f)\Big)(r,\theta)$$

where by $\mathcal{F}_2$, $\mathcal{F}_1$ we denote the two and one-dimensional Fourier transform, respectively.

Remark 6.1.2. Essentially, what we are saying by this is that if we take the one dimensional Fourier transform of the Radon transform of f with respect to t, we get the same result as when we take a two-dimensional Fourier transform of the initial function f. Figure 6.1 explains this situation.

Proof. Let us start from the right-hand side of the equation.

$$\mathcal{F}_1\mathscr{R}f(r,\theta) = \int_{\mathbb{R}} \mathscr{R}f(t,\theta)e^{-itr}\,\mathrm{d}t = \int_{\mathbb{R}} \Big(\int_{\mathbb{R}} f(t\cos\theta - s\sin\theta, t\sin\theta + s\cos\theta)\,\mathrm{d}s\Big)e^{-itr}\,\mathrm{d}t$$

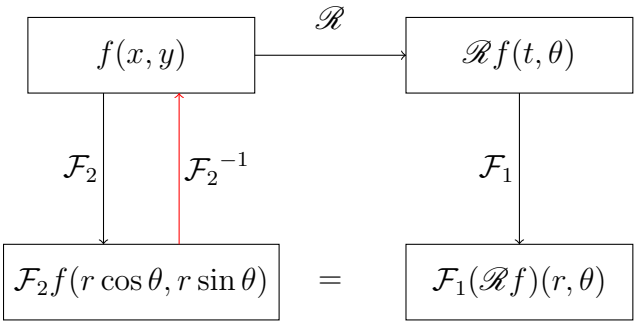

Figure 6.1: The idea of the Central Slice theorem

We are going to change the coordinates to the Cartesian ones and make a substitution. We know that

$$\begin{pmatrix} x \\ y \end{pmatrix} = \begin{pmatrix} \cos\theta & -\sin\theta \\ \sin\theta & \cos\theta \end{pmatrix} \begin{pmatrix} t \\ s \end{pmatrix}$$

By calculus substitution theorem, we need to compute the determinant of our Jacobi matrix, which is given by

$$J = \begin{pmatrix} \frac{\partial x}{\partial t} & \frac{\partial x}{\partial s} \\ \frac{\partial y}{\partial t} & \frac{\partial y}{\partial t} \end{pmatrix} = \begin{pmatrix} \cos\theta & -\sin\theta \\ \sin\theta & \cos\theta \end{pmatrix}$$

We observe that the Jacobi matrix is the known rotation matrix, whose determinant is 1 so we have

$$\mathrm{d}x\,\mathrm{d}y = \mathrm{d}s\,\mathrm{d}t$$

Moreover, we can use the fact that the inverse of the rotation matrix is equal to its transpose, which yields

$$\begin{pmatrix} t \\ s \end{pmatrix} = \begin{pmatrix} \cos\theta & \sin\theta \\ -\sin\theta & \cos\theta \end{pmatrix} \begin{pmatrix} x \\ y \end{pmatrix}$$

and we see that

$$t = x\cos\theta + y\sin\theta$$

Going back to the integral, we get

$$\int_{\mathbb{R}^2} f(x,y) e^{-i(x\cos\theta + y\sin\theta)r}\,\mathrm{d}x\,\mathrm{d}y$$

On the other hand, if we look at the definition of the two-dimensional Fourier transform

of f, for some $\boldsymbol{\alpha} = (\alpha_1, \alpha_2)$, we have

$$(\mathcal{F}_2 f)(\alpha_1, \alpha_2) = \int_{\mathbb{R}^2} f(x, y) e^{-i(x\alpha_1 + y\alpha_1)} \, \mathrm{d}x \, \mathrm{d}y$$

Since we want our two-dimensional Fourier transform evaluated at $(r\cos\theta, r\sin\theta)$, we put

$$\alpha_1 = r\cos\theta$$

$$\alpha_2 = r\sin\theta$$

which proves the equality. ■

6.2 The meaning of the Central slice theorem

Let us now explain this in greater detail. As we have already stated in the definition of the Radon transform in Chapter 4, the Radon transform is actually a *slice* that we get for a fixed angle θ and many values of t; often being called *projection*. When we do the one-dimensional Fourier transform of this projection with respect to t, we get the function that depends on r and θ. This value is denoted as $\mathcal{F}_1(\mathscr{R}f)(r, \theta)$, it is the same as the value of *slice* of a two-dimensional Fourier transform of our initial function taken at angle θ and different values of r. Since the $\mathcal{F}_2$ is being evaluated at $(r\cos\theta, r\cos\theta)$, which are well-known polar coordinates, we observe that, for a fixed angle θ, as we move with the radius r in the space where our $\mathcal{F}_2 f$ lives, we get the same value for a fixed θ by varying the r in the space where our $\mathcal{F}_1(\mathscr{R}f)$ live [17]. For a better understanding of this idea, see Figure 6.2.

We take some fixed angle θ_i, then get the *projection* (marked red in the upper left corner), do the Fourier transform of this projection, and get the result marked by a red line to the right. On the other side, we take the function, do its two-dimensional Fourier transform (marked pink on the right side), and "slice it" under the angle of θ_i. The result is again the red line on the right.

The theorem is, for obvious reasons stated above, often called *Fourier-slice theorem* and *Projection-slice theorem* too.

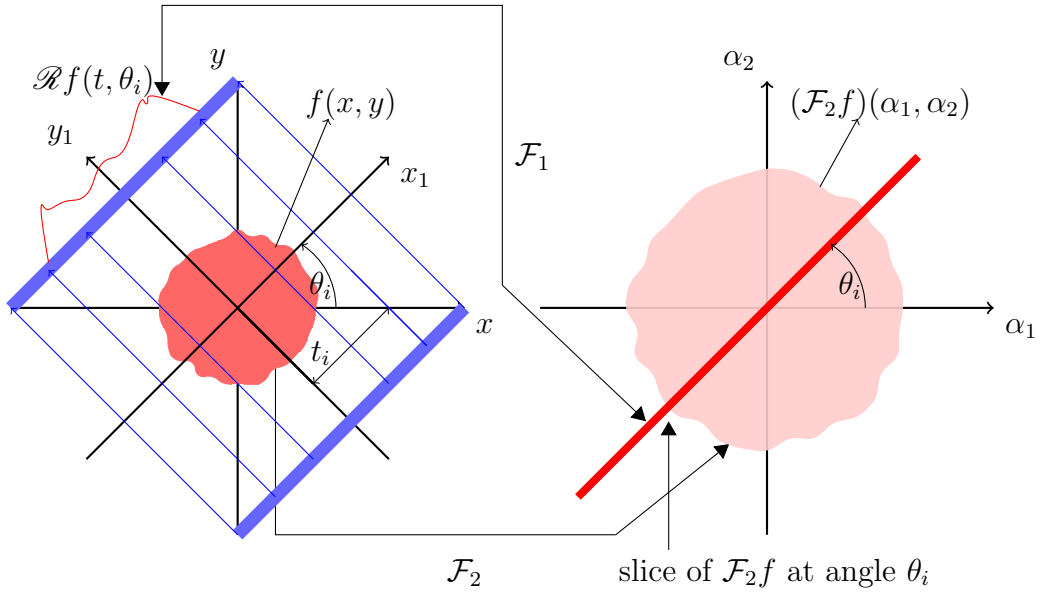

Figure 6.2: Illustration of the Central slice theorem

Chapter 7

Example

Now that we finally know how to compute the inversion of the Radon transform, we will show all of the facts stated earlier on a simple example.

Reconstruction of the cylinder Assume we have a two-dimensional cylinder function, that is, we have the following information:

$$a(x,y) = \begin{cases} 1, & x^2 + y^2 \leq 1 \\ 0, & \text{otherwise} \end{cases}$$

where $a(x,y)$ is our *attenuation coefficient*. To have a better idea what our function looks like, see Figure 7.1. For plotting all of the graphs that follow, we will use *Wolfram Mathematica* software.

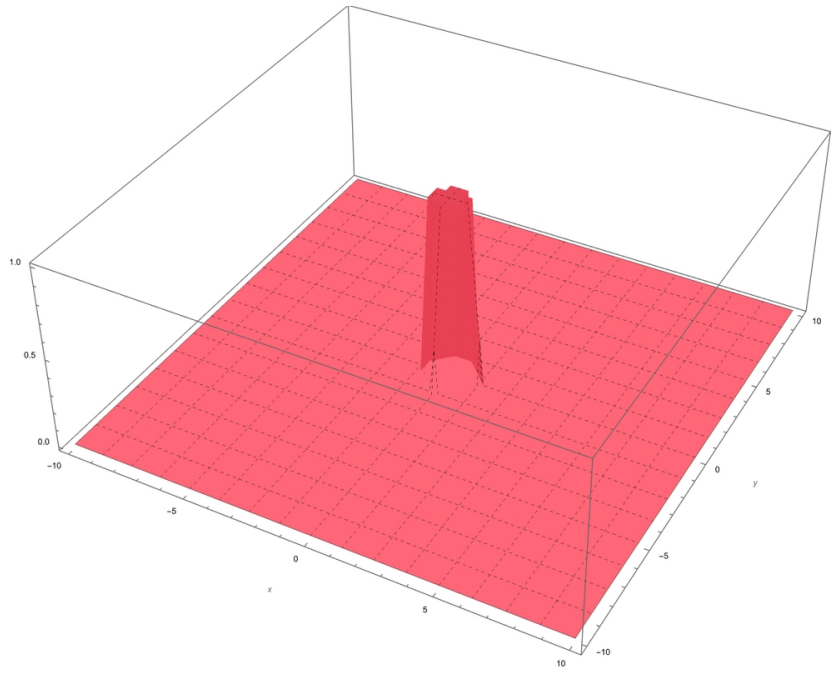

Figure 7.1: The Cylinder function

Our first step is to compute the Radon transform of the given function. From the notation of Chapter 4, we have

$$x^2 + y^2 = (t\cos\theta - s\sin\theta)^2 + (t\sin\theta + s\cos\theta)^2 = t^2 + s^2$$

Therefore, we have

$$a(s) = \begin{cases} 1, & -\sqrt{1-t^2} \le s \le \sqrt{1-t^2} \\ 0, & \text{otherwise} \end{cases}$$

$$\mathscr{R}a(t,\theta) = \int_{-\sqrt{1-t^2}}^{\sqrt{1-t^2}} \mathrm{d}s = 2\sqrt{1-t^2}$$

The Radon transform is

$$\mathscr{R}a(t,\theta) = \begin{cases} 2\sqrt{1-t^2} & |t| \le 1 \\ 0 & |t| \ge 1 \end{cases}$$

We notice right at the beginning that the Radon transform does not depend on the angle. That means that the function has a certain symmetry and it looks "the same" for any value of θ.

On Figure 7.2 we can see the Radon transform $\mathscr{R}a(t,\theta)$ of $a(x,y)$.

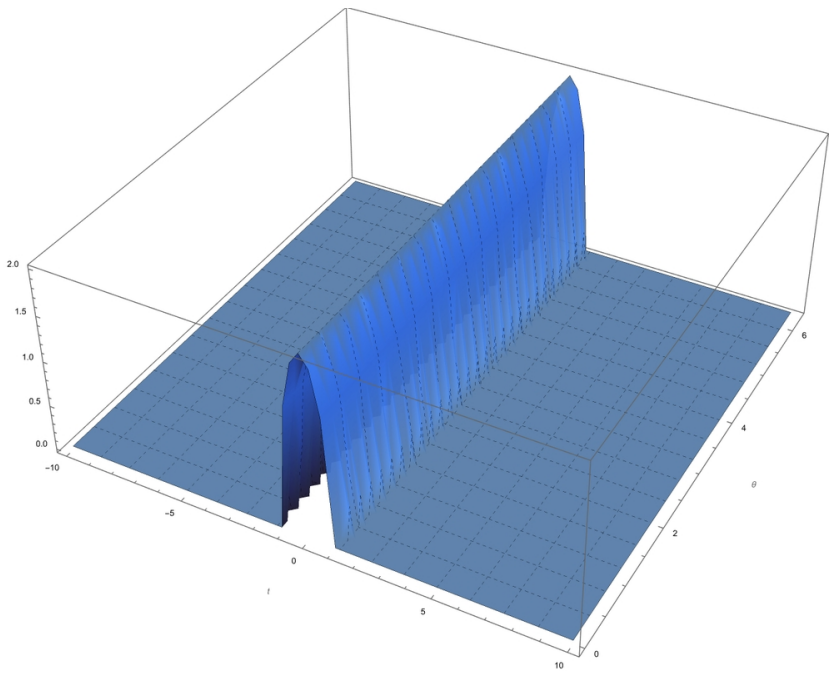

Figure 7.2: The Radon transform of the cylinder function

Next step is to compute the one-dimensional Fourier transform of the obtained Radon transform. We compute the Fourier transform with respect to t for a fixed angle θ. From

the definition of the Fourier transform, we get the following:

$$\mathcal{F}_1\{\mathscr{R}a(t,\theta)\} = \frac{1}{2\pi}\int_{-1}^{1} 2\sqrt{1-t^2}\cdot e^{-itr}\,\mathrm{d}t$$

Unfortunately, the above obtained integral is slightly complicated, as it requires the introduction of some non-trivial integrals in its solution. Because of this, we have used the software *Wolfram Mathematica* to evaluate it. It gave us following results:

$$\mathcal{F}_1(\mathscr{R}a)(r,\theta) = \frac{J_1(r)}{r} \tag{7.1}$$

Observe that the software had introduced a new special function J_1, called the first Bessel function of the first kind. We now see that even the simplest function requires non-trivial computations. In fact, Bessel functions arise whenever the body we scan has a rotational symmetry, which our cylinder certainly does have (we can observe this from the graph). Another way then using software for this computation, we can look at the integral table of Fourier transform, which can be found in Appendix A of the book [23]. In Figure 7.3 we have plotted the one-dimensional Fourier transform. Additionally, on

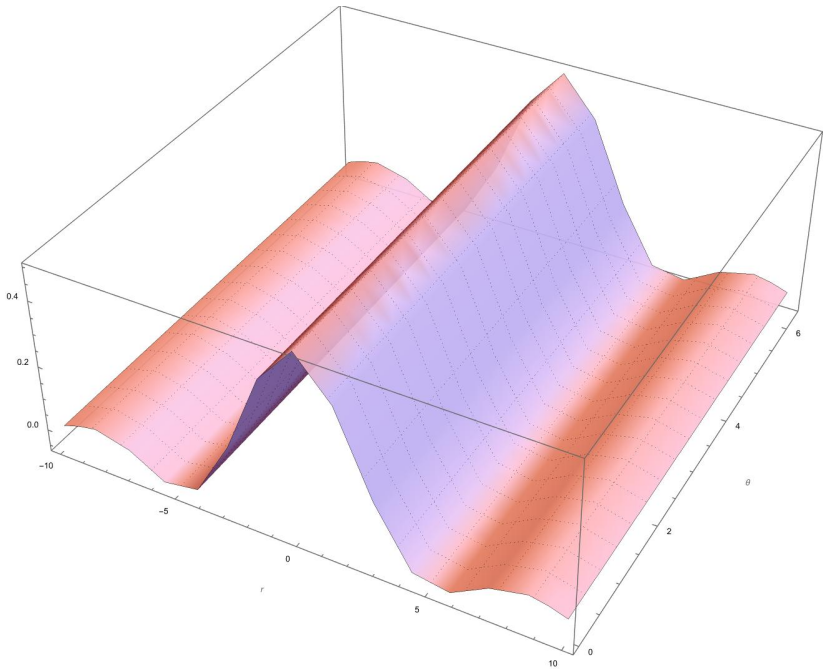

Figure 7.3: The one-dimensional Fourier transform of the Radon transform

Figure 7.4 we can see how the "slices" of the Radon and the Fourier transform transform look in the plane, for some arbitrary value of θ.

In the Central slice theorem, we have proved that, by taking a two-dimensional Fourier transform of the initial function $a(x,y)$, we should get the result obtained in the equa-

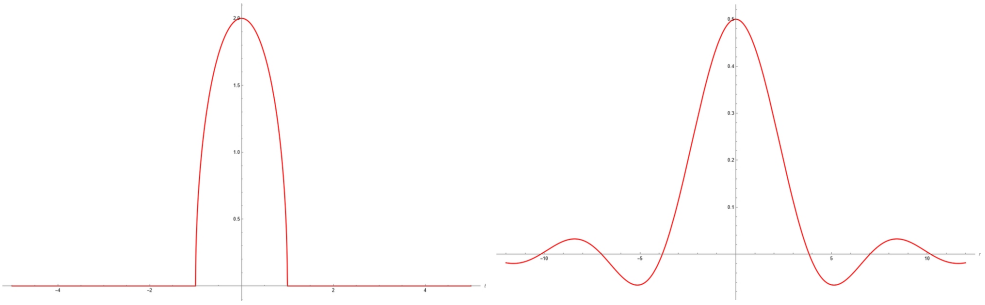

Figure 7.4: Radon Transform and 1D Fourier transform in plane

tion (7.1). Let us show that this indeed does hold for our function.

First of all, we will pass from Cartesian to the polar coordinates[1]:

$$x = \hat{r}\cos\varphi$$

$$y = \hat{r}\sin\varphi$$

$$\hat{r} \in \mathbb{R} \qquad \varphi \in |0, 2\pi)$$

Our function will then be

$$a(\hat{r}, \varphi) = \begin{cases} 1, & 0 \leq \hat{r} \leq 1 \\ 0, & \text{otherwise} \end{cases}$$

Now we will compute the Fourier transform of $a(\hat{r}, \varphi)$. We observe that the above stated function is so-called *separable function*,which is a function of two variables that can be represented as a product of two functions that depend on one variable only [12]. Therefore, we can write it as follows:

$$a(\hat{r}, \varphi) = a_1(\hat{r}) \cdot a_2(\varphi)$$

A general form of two-dimensional Fourier transform of our function in Cartesian coordinates

$$\{\mathcal{F}_2 a(x, y)\}(\alpha_1, \alpha_2) = \frac{1}{2\pi} \int_{\mathbb{R}^2} a(x, y) e^{-i(x\alpha_1 + y\alpha_2)} \, \mathrm{d}x \, \mathrm{d}y$$

can be rewritten as follows:

$$x = \hat{r}\cos\varphi \qquad \alpha_1 = \rho\cos\psi$$

$$y = \hat{r}\sin\varphi \qquad \alpha_2 = \rho\sin\psi$$

$$\hat{r}, \rho \in \mathbb{R} \qquad \varphi, \psi \in |0, 2\pi)$$

[1] By passing to the polar coordinates, the circular symmetry that we have mentioned earlier gets more obvious.

hence

$$x\alpha_1 + y\alpha_2 = \hat{r}\rho(\cos\varphi\cos\psi + \sin\varphi\sin\psi) = \hat{r}\rho\cos(\varphi - \psi)$$

Moreover, we have

$$\mathrm{d}x\,\mathrm{d}y = \hat{r}\,\mathrm{d}\hat{r}\,\mathrm{d}\varphi$$

We obtain

$$\begin{aligned}\frac{1}{2\pi}\int_{\mathbb{R}^2} a(x,y)e^{-i(x\alpha_1+y\alpha_2)}\,\mathrm{d}x\,\mathrm{d}y &= \frac{1}{2\pi}\int_0^{2\pi}\int_0^{\infty} a(\hat{r},\varphi)e^{-i\hat{r}\rho\cos(\varphi-\psi)}\hat{r}\,\mathrm{d}\hat{r}\,\mathrm{d}\varphi \\ &= \frac{1}{2\pi}\int_0^{\infty}\hat{r}a_1(\hat{r})\Big(\int_0^{2\pi} a_2(\varphi)e^{-i\hat{r}\varphi\cos(\varphi-\psi)}\,\mathrm{d}\varphi\Big)\,\mathrm{d}\hat{r}\end{aligned}$$

Since our function depends only on $\hat{r}$, $a_2(\varphi) = 1$ for all $\varphi \in \mathbb{R}$. Further on, we have:

$$\int_0^{\infty}\hat{r}a_1(\hat{r})\Big(\frac{1}{2\pi}\int_0^{2\pi} e^{-i\hat{r}\rho\cos(\varphi-\psi)}\,\mathrm{d}\varphi\Big)\,\mathrm{d}\hat{r}$$

Since cosine is a periodic function, and we are integrating over one period only the value of the middle integral is:

$$\frac{1}{2\pi}\int_0^{2\pi} e^{-i\hat{r}\rho\cos\varphi}\,\mathrm{d}\varphi = \frac{1}{2\pi}\int_{-\pi}^{\pi} e^{-i\hat{r}\rho\sin\varphi}\,\mathrm{d}\varphi = J_0(\hat{r}\rho)$$

where $J_0(\hat{r}\rho)$ is by the definition the 0-th Bessel function of the first kind (See [14]). Further on, we have

$$\int_0^{\infty}\hat{r}a_1(\hat{r})J_0(\hat{r}\varphi)\,\mathrm{d}\hat{r} = \int_0^1 \hat{r}J_0(\hat{r}\rho)\,\mathrm{d}\hat{r}$$

where we have used the fact that

$$a_1(\hat{r}) = a(\hat{r}) = \begin{cases}1, & 0 \le \hat{r} \le 1\\ 0, & \text{otherwise}\end{cases}$$

Now we will make a substitution

$$\hat{r}\rho = u$$

$$\rho\,\mathrm{d}\hat{r} = \mathrm{d}u$$

$$\int_0^{\rho}\frac{u}{\rho}J_0(u)\frac{\mathrm{d}u}{\rho} = \frac{1}{\rho^2}\int_0^{\rho} uJ_0(u)\,\mathrm{d}u = \frac{1}{\rho^2}\cdot\rho\cdot J_1(\rho) = \frac{J_1(\rho)}{\rho} \tag{7.2}$$

where we have used the recurrence relation for Bessel functions (See [23]):

$$\frac{\mathrm{d}}{\mathrm{d}x}(x^nJ_n(x)) = x^nJ_{n-1}(x)$$

If we look at the Central slice theorem again, we want to evaluate the result obtained in equation (7.2) at $(\alpha_1, \alpha_2) = (r\cos\theta, r\sin\theta)$. However, the function does not depend on the angle, so we will have:

$$\{\mathcal{F}_2 a(x,y)\}(r,\theta) = \{\mathcal{F}_2 a(x,y)\}(r) = \frac{J_1(\rho)}{\rho}\bigg|_{\rho=r} = \frac{J_1(r)}{r}$$

which is exactly the result we obtained in the equation (7.1).

We can conclude that the approach to the reconstruction process that the Central slice theorem gives us produces complicated computations even for the most straightforward functions. Nevertheless, the theorem results represented an important starting point for other image reconstruction techniques, that we mention briefly in Conclusion.

Chapter 8

Conclusion

This thesis aimed to explain the fundamental mathematical principles used in image reconstruction. Although we primarily focused on medical image reconstruction, more precisely, on X-ray tomography, there are other medical imaging techniques that use those principles as well, such as SPECT (single photon emission tomography), PET (positron emission tomography), or MRI (magnetic resonance imaging) [13]. Even though *tomography* and the use of Radon transform have the most prominent significance in medicine, they are important and valuable in other fields too.

In **Chapter 2**, we discussed how a CT scanner works and what tomography is, and we gave a mathematical model that explains X-rays traveling through an object (such as a bone), which we created using Beer's law.

After having an adequate mathematical model, we had to describe our coordinate system in a suitable way, which is what we have done in the **Chapter 3**. The so-called *Space of lines in plane* describes lines in terms of an angle and afine parameter, which significantly simplifies the whole reconstruction problem.

After making the mathematical model and proper representation of lines in plane, we were finally able to define the Radon transform and see exactly why the inverse Radon transform is our goal when it comes to function reconstruction. We described this in **Chapter 4**.

Since the inversion of the Radon transform is neither straightforward nor somewhat trivial, in **Chapter 5** have we talked about Fourier analysis which plays a central role in the reconstruction process that we are explaining in the thesis.

In **Chapter 6**, we have come to the main goal of the thesis, which is to prove the *Central slice theorem*. This theorem shows us one of the ways to recover the initial function and reconstruct the body. After proving the theorem, we built all of the essential theoretical knowledge, which we then applied in the simple example in **Chapter 7**. In this example, we have seen that even for a relatively simple function, the reconstruction process done

through the *Central slice theorem* gives us some complicated integrals that we can not solve without integral tables or some mathematical software. At the end of the reconstruction process, we got the two-dimensional slices as our wanted result (the ones showed in the Figure 4.3), but one may ask, how do we get the three-dimensional reconstruction (as one showed in Figure 4.2)? One way to do this is to stack the 2D slices at many different heights in the three-dimensional space. The other way is to extend the two-dimensional technique only to a higher dimension. Instead of measuring an X-ray beam along the line, the X-ray flux is being measured on the plane. The three-dimensional projection is obtained as the intersection of two planes. Because the beams are recreated in a cone form, the method is called Cone beam reconstruction [16].
Throughout the thesis, we are talking only about the "continuous world", which gives us the exact results in theory but is not feasible in real-life situations. To talk about the real-life applications means to talk about the "discrete world". Some methods used in the "discrete world" are developed analogously to the continuous ones, such as the Direct Fourier method (the Central slice method we are talking about in the thesis). More information about the algorithm that describes this method numerically can be found in the book [24]. Considering the complexity of computations of the Central slice theorem method, it is rarely used. Other techniques that give better results are developed, such as *Signal space convolution and frequency space filtering*, *Iterative methods* or *Series methods and orthogonal functions* [7]. More information about more efficient numerical methods can be found in, for example, the book [2].

Even though none of the theoretical techniques that we have explained in the thesis are used practically in the same form, they are of enormous significance because they represent a basis and one of the starting points for image reconstruction processing. If we want to have a complete picture and completely understand the numerical methods being used, we first need to understand the mathematical theory behind it. Accordingly, our plans for future research can be based on numerical algorithms that are used in practice.

Bibliography

[1] Robert Alexander Adams and Christopher Essex. *Calculus: A Complete Course*. Reading, MA, USA: Addison-Wesley, 1999.

[2] Guillaume Bal and Philippe Moireau. "Fast numerical inversion of the attenuated Radon transform with full and partial measurements". In: *Inverse Problems* 20.4 (2004), p. 1137.

[3] Daniel Balbachevsky et al. "Combination of Anterior and Posterior Subcutaneous Internal Fixation for Unstable Pelvic Ring Injuries: The". In: *Journal of Trauma and Injury* 32.1 (2019), pp. 51–59.

[4] *Basic principles of Computed Tomography and relevant neuroanatomy*. (Accessed on 01.02.2022). URL: http://www.southsudanmedicaljournal.com/archive/august-2016/how-to-interpret-an-unenhanced-ct-brain-scan.-part-1-basic-principles-of-computed-tomography-and-relevant-neuroanatomy.html.

[5] Jen Beatty. "The Radon transform and the mathematics of medical imaging". In: (2012).

[6] Kailley Bolles. "Mathematics of medical imaging". In: *Inverting the Radon transform* (2011).

[7] Stanley R Deans. *The Radon transform and some of its applications*. Courier Corporation, 2007.

[8] Roland Dobbs. *Electromagnetic waves*. Springer Science & Business Media, 2013.

[9] Charles L. Epstein. *Introduction to the mathematics of medical imaging*. Society for Industrial and Applied Mathematics, 2008.

[10] Timothy G. Feeman. *The mathematics of medical imaging: a beginner's guide*. New York: Springer, 2009.

[11] Joseph Fourier et al. *The analytical theory of heat*. The University Press, 1878.

[12] *Fundamentals of Diffraction and Image Formation*. (Accessed on 13.05.2022). 2007. URL: http://www.optique-ingenieur.org/en/courses/OPI_ang_M02_C01/co/Contenu_03.html.

[13] Rafael C Gonzalez and Richard E Woods. *Digital Image Processing, Hoboken*. 2018.

[14] Robert M Gray and Joseph W Goodman. *Fourier transforms: an introduction for engineers*. Vol. 322. Springer Science & Business Media, 2012.

[15] *Introduction to a line integral of a scalar-valued function*. (Accessed on 14.04.2022). URL: http://mathinsight.org/line_integral_scalar_function_introduction.

[16] Avinash C Kak and Malcolm Slaney. *Principles of computerized tomographic imaging*. SIAM, 2001.

[17] Robert M Lewitt. "Reconstruction algorithms: transform methods". In: *Proceedings of the IEEE* 71.3 (1983).

[18] Johann Radon. "Über die bestimmung von funktionen durch ihre integralwerte längs gewisser mannigfaltigkeiten". In: *Classic papers in modern diagnostic radiology* (2005).

[19] Walter Rudin. *Real and complex analysis*. English. 1st ed. N.York: Osborne-McGraw-Hill, 1966.

[20] *Saving lives: the mathematics of tomography*. (Accessed on 09.02.2022). Internet Engineering Task Force, 2008. URL: https://plus.maths.org/content/saving-lives-mathematics-tomography.

[21] Robert S Strichartz. *A guide to distribution theory and Fourier transforms*. World Scientific Publishing Company, 2003.

[22] Paul Suetens. *Fundamentals of medical imaging*. Cambridge university press, 2017.

[23] Nico M Temme. *Special functions: An introduction to the classical functions of mathematical physics*. John Wiley & Sons, 1996.

[24] Dominique Zosso, CM Bach, and Jean-Philippe Thiran. "Direct fourier tomographic reconstruction image-to-image filter". In: *Insight Journal* (2007), pp. 1–13.